A Multivariate Stochastic Volatility Model Based on Generalized Factor Dynamics

João Pedro Coli de Souza Monteneri Nacinben[†]
João Pedro Malim Franco[‡]
Márcio Laurini[*]
Pedro Chaim[**]

Abstract

In this work we introduce a new class of multivariate stochastic volatility models using a latent multifactor structure. Latent factors can follow distinct dynamic structures - stationary autoregressive processes, first- and second-order random walks, and long memory processes. The combination of different dynamic structures in the latent factors makes it possible to capture short and long memory processes, and also the impact of shocks with permanent effects on the conditional variance structure. We perform Bayesian inference of parameters, latent factors and predictions using Bayesian estimation using Integrated Nested Laplace Approximations (INLA), making the method computationally efficient and scalable. We applied this method to analyze a portfolio of cryptocurrencies, and the results of the in-sample and out-of-sample analyzes indicate the importance of combining short- and long-memory processes to capture the dynamics of this market.

Keywords: Multivariate Stochastic Volatility; Factor Models; fractional Gaussian Noise; Splines; Forecasting.
JEL Code: 31; 34.

1. Introduction

Multivariate conditional variance models hold significant importance in financial applications due to their ability to capture and analyze the complex interrelationships among multiple assets. This class of models allows analysts and investors to better understand and manage risks by considering the correlations and dependencies between different assets. By incorporating these in

[†]Department of Economics, FEARP-University of São Paulo, Brazil: joao.nacinben@alumni.usp.br
[‡]Department of Economics, FEARP-University of São Paulo, Brazil: joaopfranco@usp.br
[*]Department of Economics, FEARP-University of São Paulo, Brazil: laurini@fearp.usp.br
[**]Department of Economics, Federal University of Santa Catarina, Brazil: pedro.chaim@ufsc.br

their models, risk managers are able to more accurately assess the overall risk exposure of a portfolio and take appropriate measures to mitigate it.

Multivariate conditional variance models enable investors to construct diversified portfolios that are resilient to adverse market movements, and play a crucial role in developing effective hedging strategies by identifying the relationships between different assets and their volatilities. Accurate forecasting of future volatility is essential for risk management and trading strategies. Multivariate conditional variance models help in forecasting the future volatility levels of multiple assets or variables, providing valuable insights for decision-making purposes. By incorporating these forecasts into their models, investors and traders can better anticipate market trends and adjust their strategies accordingly.

An important class of conditional volatility models focuses on treating conditional volatility as a stochastic process, commonly known as stochastic volatility (SV) models. Initially introduced by Taylor (1986), these models utilize a nonlinear state-space framework, where the log-variance follows an first-order autoregressive AR(1) process. Univariate SV models offer several advantages over the alternative class of univariate ARCH class, introduced by Engle (1982). They do not require assuming a deterministic structure for latent variance, as assumed by the ARCH class of models, and by employing autoregressive formulations for the conditional variance, they facilitate a more straightforward extension to the multivariate realm. This extension can be achieved through formulations based on vector autoregressive (VAR) models and common factor structures. However, it is important to note that SV models entail greater complexity in their estimation due to the presence of latent variables in the likelihood of the process.

The estimation of stochastic volatility models requires the treatment of the latent variances in the inference procedures. The inference method proposed by Taylor (1986) for the estimation of SV models is based on the method of moments, but this method only permits to estimate the fixed parameters of the process and does not allow the estimation of the latent variance of the process. Generalized Method of Moments estimation of SV models was proposed by Andersen and Sorensen (1996), but this approach presents a relevant bias in finite samples and is also not very robust to outliers and other forms of process contamination, as discussed by Laurini and Hotta (2017), which present an alternative estimation based on generalized empirical likelihood and minimum contrast to solve the bias and robustness problems linked to estimation by the generalized moments method in the estimation of SV models.

In the realm of frequentist methodology, a notable advancement lies in the quasi-maximum likelihood approach, which utilizes prediction error de-

composition through the Kalman Filter using state space representations. This method, independently introduced by Nelson (1988) and Harvey et al. (1994), has garnered significant attention. On the other hand, Bayesian estimation techniques offer an intriguing alternative, enabling the treatment of latent processes as additional hyperparameters in the estimation procedure. The original Bayesian inference for SV models was presented by Kim and Shephard (1998), while more recent contributions, such as those by Kastner and Frühwirth-Schnatter (2014), delve into this domain, employing Markov Chain Monte Carlo (MCMC) algorithms for estimation.

Martino et al. (2011) introduce an alternative Bayesian estimation approach for stochastic volatility models utilizing integrated nested Laplace approximations (INLA), originally introduced by Rue et al. (2009). This methodology facilitates the estimation of parameters and latent variables through accurate deterministic approximations to posterior distributions, assuming that the model can be approximated by a Gaussian Markov random field. Significantly, Chaim and Laurini (2019a) emphasizes that the INLA method, founded on an analytical framework, obviates the necessity for simulation procedures, consequently also eliminating concerns regarding chain convergence issues.

Since the introduction of stochastic volatility models by Taylor (1986), numerous extensions have emerged, offering a broader range of specifications and enabling the analysis of conditional volatility patterns in multivariate settings. Following the pioneering work of Harvey et al. (1994), multivariate stochastic volatility (SV) modeling has gained traction and undergone further refinement, incorporating appropriate functional forms to capture specific stylized facts and presenting more efficient approaches to estimation and parameterization.

Within this evolving landscape, the concept of factor structures has been introduced into multivariate stochastic volatility modeling, with notable emphasis provided by Jacquier et al. (1995). These factor structures aim to tackle the computational complexities associated with the inherent high dimensionality of multivariate volatility modeling.

The foundational work of Harvey et al. (1994) laid the groundwork for what they termed as a multivariate generalization of stochastic variance models. Factor models moving in the same direction is the class of multiplicative models, partly inspired by the work of Quintana and West (1987). Asai et al. (2006) discuss four alternative formulations for MSV models, based on exponential matrix transformation, Cholesky decomposition, Wishart autoregressive process and the observed variation (*range*).

Nacinben and Laurini (2024) introduce a multivariate stochastic volatility

(MVSV) model with latent common factors which can be efficiently estimated using INLA, proposing a computationally efficient approach for estimating multivariate stochastic volatility models. The methodology leverages sparse linear algebra and parallelization techniques.

Their formulation is flexible in that the number of latent factors can be determined via traditional information criteria and is parsimonious when compared to popular existing multivariate stochastic volatility and GARCH-based models. Furthermore, because INLA is an analytical method of Bayesian estimation, the procedure avoids issues with MCMC chain convergence. They provide a comparative analysis with MSV models estimated using MCMC, demonstrating the computational efficiency and goodness of fit improvements achieved with the new approach.

One relevant limitation of this model, however, is that all latent common factors follow AR(1) processes. Here we propose an extension to the model of Nacinben and Laurini (2024) in which each common latent factor may follow a different stochastic processes. Our formulation allows each latent factor to be represented by processes with different dynamics. In particular we allow the latent common factors to assume dynamics given by stationary first order autoregressive processes (AR(1)), first order random walks (RW1), second order random walks (RW2), which are equivalent to spline models, and also long memory processes, using a representation based on fractional Gaussian noise (fGn).

This structure allows the multivariate stochastic volatility process to capture short (AR(1)) and long (fGn) memory structures, the impact of shocks with permanent effects (RW1) and the effect of permanent shocks that smoothly change the level of volatility (RW2), a characteristic analogous to the so-called spline-GARCH model of Engle and Rangel (2008).

The RW2 model finds widespread utility in statistical applications, particularly in tasks such as data smoothing and modeling response functions. These methods, including semi-parametric regression, smoothing, and penalized likelihood (e.g., (Rue and Held, 2005)). The RW2 process is also connected to spline smoothing methods, where smoothing is obtained by penalizing the second derivative of the function. As we can approximate the second derivative by the iterated application of finite differences (the difference of the difference), we have the relationship between the process RW2, which is given is a process where the second difference is an independent Gaussian process, and the principle of smoothing by functions smooth (splines), which are functions with limited curvature (second derivative). Spline smoothing methods are used in finance to smooth the yield curve ((Vasicek and Fong, 1982)), but but also find applications in modeling conditional volatility.

The spline-Garch model proposed by (Engle and Rangel, 2008) decomposes the conditional volatility in two components, a slow movement component, represented by exponential splines, and a GARCH process. The spline component captures smooth variations with permanent effects on the level of conditional volatility, and can also be thought of as a way to incorporate a smooth variation structure in the unconditional volatility of the process.An general approach for the application of splines in modeling conditional volatility is proposed in (Audrino and Bühlmann, 2009), using the theory of B-splines, and other applications of B-splines in modeling implied volatility in derivative prices can be found in (Fengler, 2009) and (Laurini, 2011). Our use of RW2 can be understood as a non-parametric approach to model permanent variations in unconditional volatility, capturing persistent changes in volatility patterns.

The introduction of long memory components introduces a relevant difficulty in model representation and inference procedures. Long memory processes, such as fractional Gaussian noise, are non-Markovian and non-Semi martingales (Bayer et al., 2020). The representation and inference structure using Laplace approximations is based on the Gaussian Markov Random Fields class, and in this aspect the introduction of long memory processes would initially not allow the use of the INLA method in inference procedures, as discussed for example in Chaim and Laurini (2019a).

To overcome this limitation we use a representation of fractional Gaussian noise proposed in Sørbye et al. (2017). This representation is based on the approximation of the fractional Gaussian noise using a mixture of autoregressive processes, where the mixture weights are calibrated in order to reproduce the correlation structure of the fGn process. This allows us to approximate this process as a Gaussian Markov Random Field, and thus use the representation and inference methods using Integrated Nested Laplace Approximations. This form of approximation was proposed for the estimation of univariate SV models with long memory in Chaim and Laurini (2019a), and generalized for multifactor term structure models in Valente and Laurini (2024). These two works discuss the properties of this approach, showing excellent qualities in terms of in-sample fit and forecasting for finance processes.

Long memory volatility processes are also related to the so-called processes of trending fractional volatility (Comte and Renault, 1998; Comte et al., 2012; Alòs and Yang, 2017), which is based on fractional Brownian motion models with Hurst parameter $H > 0.5$, and rough volatility processes, which correspond to processes with a Hurst parameter with $H < 0.5$, as analyzed in Gatheral et al. (2018) and Bayer et al. (2020). The methodology

proposed in this article can be used to estimate trending fractional volatility composed of multiple latent factors with distinct Hurst coefficients.

Due to the computational efficiency of the Bayesian inference method used in estimation, it is possible to carry out model selection procedures using in- and out-of-sample adjustment metrics, as well as Bayesian information criteria. The method also allows obtaining the posterior distribution of parameters, latent factors and conditional variances within and outside the sample (forecasting).

To evaluate the empirical performance of the models, we analyzed a set of five cryptocurrencies: Bitcoin (BTC), Etherium (ETH), Ripple (XRP), Solana (SOL) and Binance Coin (BNB), comparing 70 different model specifications representing combinations of models with 1, 2, 3 and 4 latent factors, and possible combinations of different possible dynamics for each latent factor (AR(1), RW1, RW2 and fGn). We compare these models using information criteria and in- and out-of-sample fit metrics, and we also build a model confidence set for the best models in the out-of-sample predictive analysis.

The results obtained indicate that the combination of distinct processes for latent factors is fundamental for gains in predictive fit, and our results indicate a special role for long memory processes in the joint dynamics of conditional variance in the cryptocurrency market.

2. Materials and Methods

2.1 The Multifactor SV model of Nacinben and Laurini (2024) and the INLA method

Our basic specification for the multifactor representation used to represent multivariate stochastic volatility models is based on the framework proposed in Nacinben and Laurini (2024). We first present this model. The model proposed by Nacinben and Laurini (2024), for m series and k latent factors, is represented as follows:

$$\mathbf{r_t} = \boldsymbol{\Omega}_t \boldsymbol{\varepsilon}_t, \quad \boldsymbol{\varepsilon}_t \sim N(\mathbf{0}, \Sigma_\varepsilon) \tag{1}$$

$$\boldsymbol{\sigma}_t = \boldsymbol{\mu} + \boldsymbol{\gamma}\mathbf{h_t} + \boldsymbol{\eta}_t, \quad \boldsymbol{\eta}_t \sim N(\mathbf{0}, \Sigma_\eta), \tag{2}$$

with $\boldsymbol{\sigma}_t = (\sigma_{1t}, \ldots, \sigma_{mt})'$ representing a vector containing the m log volatilities, $\boldsymbol{\mu} = (\mu_1, \ldots, \mu_m)'$ denotes the mean parameters, and $\boldsymbol{\gamma}$ is a $m \times k$ matrix of factor loadings. Diagonal covariance matrices Σ_ε and Σ_η are assumed for the latent factors, indicating independent stochastic volatility processes.

In the model of Nacinben and Laurini (2024) the factor log volatilities, denoted by $\mathbf{h_t} = (h_{1t}, \ldots, h_{kt})'$ follow first-order autoregressive process

$$\mathbf{h_t} = \boldsymbol{\Phi}(\mathbf{h_{t-1}}) + \boldsymbol{\xi}_t, \quad \boldsymbol{\xi}_t \sim N(\mathbf{0}, \Sigma_h), \tag{3}$$

where $\boldsymbol{\Phi} = \text{diag}(\phi_1, \ldots, \phi_k)$ is a diagonal matrix of persistence parameters, with a univariate first-order autoregressive structure for each factor. The relationship between the equations for the observed returns, represented by the vector $\mathbf{r_t} = (r_{1t}, \ldots, r_{mt})'$, and the variances for each asset is expressed using the matrix $\boldsymbol{\Omega}_t$ of size $m \times m$:

$$\boldsymbol{\Omega}_t = \begin{pmatrix} \exp\{\sigma_{1t}/2\} & 0 & \ldots & 0 \\ 0 & \exp\{\sigma_{2t}/2\} & \ldots & 0 \\ \vdots & \vdots & \ddots & \vdots \\ 0 & 0 & \ldots & \exp\{\sigma_{mt}/2\} \end{pmatrix}. \tag{4}$$

Our extension in relation to the Nacinben and Laurini (2024) model is to allow alternative dynamics for the latent factors, using, in addition to the AR(1) process, processes based on first and second order random walks and long memory processes using a representation of fractional Gaussian noise, as will be discussed in the next sections.

To realize the estimation procedure, we adhere to two essential identification constraints: ensuring that the count of factors doesn't surpass the count of return series ($k \leqslant m$), and fixing the load parameters (γ_{ij}) for one of these series at unity. Drawing from the methodology outlined in INLA, the model is reformulated as a Gaussian Markov random field model, following the three-stage approach as outlined by Martino (2007). The initial stage entails defining a likelihood model:

$$\pi(\mathbf{r}|\boldsymbol{\sigma}, \mathbf{h}, \theta_1) = \prod \pi(\mathbf{r_t}|\boldsymbol{\sigma}_t, \mathbf{h_t}, \theta_1), \tag{5}$$

where θ_1 is the hyperparameters vector to variance processes.

Subsequently, we proceed to model the latent fields denoted by $\boldsymbol{\sigma}_t$ and $\mathbf{h_t}$. This is followed by:

$$\boldsymbol{\sigma}_t|\mathbf{h_t}, \boldsymbol{\alpha}, \theta_2 \sim N(\boldsymbol{\alpha} + \boldsymbol{\gamma}\mathbf{h_t}, \Sigma_\eta) \tag{6}$$

$$\mathbf{h_t}|\mathbf{h_{t-1}}, \theta_3 \sim N(\boldsymbol{\Phi}\mathbf{h_{t-1}}, \Sigma_h), \tag{7}$$

with θ_2 and θ_3 serving as hyperparameter vectors linked to their corresponding covariance matrices (Σ_η and Σ_h), Gaussian prior distributions are adopted for the mean parameters ($\boldsymbol{\alpha}$), centered at zero. As illustrated by Martino et al. (2011), the average volatility can thus be integrated into the latent field by computing the following density:

$$\pi(\boldsymbol{\sigma},\boldsymbol{\alpha}|\theta_1) = \pi(\boldsymbol{\alpha})\prod_{t=1}^{T}\pi(\boldsymbol{\sigma}|\mathbf{h_t},\theta_1) \propto |\mathbf{Q}|^{1/2}\exp\left[-\frac{1}{2}(\boldsymbol{\sigma}',\boldsymbol{\alpha}')\mathbf{Q}(\boldsymbol{\sigma}',\boldsymbol{\alpha}')'\right], \tag{8}$$

where $\mathbf{Q}$ denotes the precision matrix, and $(\boldsymbol{\sigma}',\boldsymbol{\alpha}')$ represents the latent field for volatility. The sparse nature of $\mathbf{Q}$ contributes to computational efficiency, a property extensively explored by Rue and Held (2005) and Rue et al. (2009).

In the final stage, a prior $\pi(\boldsymbol{\theta})$ is established for the hyperparameter vectors $\boldsymbol{\theta} = (\theta_1, \theta_2, \theta_3)$. In this regard, the study adopts distributions as proposed by Martino et al. (2007) wherever applicable, particularly concerning parameters associated with the factor structure. However, for compatibility with the R-INLA package, the precision parameter (τ) is handled in terms of its natural logarithm (log-precision), representing a non-informative prior for precision, while the persistence parameter (ϕ) undergoes a transformation using a function defined between -1 and 1, as follows:

$$\ln(\tau_k) \sim logGamma(1,0.00005), \tag{9}$$

$$\ln\left(\frac{1+\phi_k}{1-\phi_k}\right) \sim N(0,0.15), \tag{10}$$

The prior distributions of the remaining parameters are Gaussian. Given the latent field $\mathbf{x} = (\boldsymbol{\sigma}',\boldsymbol{\alpha}')$, the estimation via INLA involves constructing an approximation for $\pi(x_t|\mathbf{r})$ from $\pi(\boldsymbol{\theta}|\mathbf{r})$ and from $\pi(x_t|\boldsymbol{\theta},\mathbf{r})$.

To derive the joint posterior distribution concerning the hyperparameters, we begin with the following Gaussian approximation for the complete conditional density of $\mathbf{x}$:

$$\tilde{\pi}_G(\mathbf{x}|\mathbf{r},\theta) = \bar{K}\exp\left\{-\frac{1}{2}(\mathbf{x}-\boldsymbol{\nu})'[\mathbf{Q}+\text{diag}(\mathbf{C})](\mathbf{x}-\boldsymbol{\nu})\right\}, \tag{11}$$

$\bar{K}$ represents a normalization constant, $\boldsymbol{\nu}$ denotes the mode of $\pi(\mathbf{x}|\mathbf{r},\theta)$, and diag$(\mathbf{C})$ represents a band matrix with a width equal to the number of series m, stemming from the Markov structure derived from the conditional density. This density can be expressed as:

$$\mathbf{C} = \begin{pmatrix} \mathbf{C_1} & \mathbf{0} & \dots & \mathbf{0} \\ \mathbf{0} & \mathbf{C_2} & \dots & \mathbf{0} \\ \vdots & & \ddots & \vdots \\ \mathbf{0} & \dots & & \mathbf{C_T} \end{pmatrix}, \tag{12}$$

where $\mathbf{C_t}$ encompasses the 2^d order terms in the Taylor expansion $\sum \log \pi(\mathbf{r_t}|x_t,\theta_1)$ around $\boldsymbol{\nu}$ within the Hessian. Consequently, the joint posterior for $\boldsymbol{\theta}$ can be approximated using the following relationship:

$$\tilde{\pi}(\boldsymbol{\theta}|\mathbf{r}) \propto \left.\frac{\pi(\mathbf{r}|\mathbf{x},\boldsymbol{\theta})\pi(\mathbf{x}|\boldsymbol{\theta})\pi(\boldsymbol{\theta})}{\tilde{\pi}_G(\mathbf{x}|\boldsymbol{\theta},\mathbf{r})}\right|_{\mathbf{x}=\boldsymbol{\nu}(\boldsymbol{\theta})}. \tag{13}$$

The approximation for $\pi(x_t|\boldsymbol{\theta},\mathbf{r})$, conversely, adopts a Gaussian approach but can leverage the outcomes derived during the evaluation stage $\tilde{\pi}(\boldsymbol{\theta}|\mathbf{r})$. Specifically, we utilize $\tilde{\pi}G(\mathbf{x}|\boldsymbol{\theta},\mathbf{r})$ as the mean parameter for the distribution, with only the values for the marginal variances, denoted by σG^2, remaining. This computation is conducted following the recursive techniques proposed by Rue and Martino (2007), facilitating the approximation to be expressed as:

$$\tilde{\pi}_G(\mathbf{x}|\boldsymbol{\theta},\mathbf{r}) = N(x_t;\boldsymbol{\nu}[\boldsymbol{\theta}],\sigma_G^2[\boldsymbol{\theta}]). \tag{14}$$

It is essential to note, as highlighted by Rue and Martino (2007), that this approximation may lack accuracy in certain scenarios, particularly when encountering extreme values for $\boldsymbol{\theta}$. Its value lies in offering a quicker alternative to more precise calculation methods, particularly beneficial in models where managing dimensionality is a significant concern.

Finally, $\pi(x_t|\mathbf{r})$ can be approximated, once $\pi(\boldsymbol{\theta}|\mathbf{r})$ and $\pi(x_t|\boldsymbol{\theta},\mathbf{r})$, through a numerical integration of the type:

$$\tilde{\pi}(x_t|\mathbf{r}) = \sum_n \tilde{\pi}(x_t|\boldsymbol{\theta}_n,\mathbf{r})\tilde{\pi}(\boldsymbol{\theta}_n|\mathbf{r})\Delta_n, \quad n \in \{1,\ldots,N\}, \tag{15}$$

To expedite the approximation process, integration is carried out over a set of points (*grid*) for $\boldsymbol{\theta}$, with equal weights Δ_n set to 1 for equidistant points. However, to enhance speed, we adopt an empirical Bayes approach, where only one integration point equivalent to the posterior mode of hyperparameters is utilized. In this approach, $\tilde{\pi}(x_t|\boldsymbol{\theta}n,\mathbf{r})$ is replaced by $\tilde{\pi}(xt|\boldsymbol{\theta},\mathbf{r})$, where $\boldsymbol{\theta}$ represents the mode of $\tilde{\pi}(\boldsymbol{\theta}|\mathbf{r})$. As stated by Martino (2007), this approach yields highly accurate results when the distribution of the hyperparameter vector conditional on the log-returns is regular.

2.2 Alternative dynamics for the latent factors

As discussed in the introduction of the article, the contribution of the present work is to extend the dynamics of latent factors to additional dynamics in the structure of an AR(1) that is used in the Nacinben and Laurini (2024) model. In addition to the AR(1) model, which is traditional in the literature of stochastic volatility models, we allow the latent factors to follow the

dynamics of first- and second-order random walk processes, as well as long-memory dynamics using a representation based on the fractional Gaussian. We detail these structures below.

2.2.1 First-order Random Walk (RW1)

The first-order Random Walk is a restriction of the autoregressive process, where we assume that the persistence coefficient ϕ is equal to one, and in this way we assume that shocks to this factor have permanent effects on the series. In this form we have that an RW1 is represented by

$$h_t = h_{t-1} + z_t, \quad z_t \sim N(0,(1\tau_{rw1})^{-1}). \tag{16}$$

In this specification, the only parameter to be estimated for this factor is the precision τ_{rw1} of the RW1 component. We assume a log-gamma prior for the precision component.

2.2.2 Second-order Random Walk (RW2)

The representation of the second-order random walk (RW2) assumes that the latent factor h_t is constructed by assuming independent second-order increments with precision τ_{rw2}. That is,

$$\Delta^2 h_t \sim N(0,1/\tau_{rw2}). \tag{17}$$

The utilization of a second-order random walk structure serves as a means to depict non-stationary processes with smooth variations and provides an alternative representation akin to spline models. This approach is prevalent in statistics, as evidenced by works such as Lindgren and Rue (2008). It's important to note that a similar relationship exists between the well-known Hodrick-Prescott (HP) filter and spline representations, a connection extensively discussed in studies like Harvey and Jaeger (1993), Harvey and Trimbur (2008) and Paige and Trindade (2010). Similar to the RW1 dynamics we assume a log-gamma prior for the precision parameter τ_{rw2}.

2.2.3 Long Memory Dynamics

While SV models effectively capture crucial characteristics of return series, such as minimal autocorrelation in levels and elevated kurtosis, they may sometimes underestimate the persistence of autocorrelation in squared returns. This discrepancy suggests the existence of long-memory dynamics in certain assets.

According to Beran (2017), a weakly stationary process has long memory if its autocovariance function $\gamma(k)$ for distant lags k satisfy

$$\gamma(k) \sim C_1 k^{2(H-1)}, \quad \text{as } k \to \infty,$$

for $C_1 > 0$, with $1/2 < H < 1$. Or, equivalently, in the frequency domain, the spectral density $f(\omega)$ for frequencies $\omega \in [-\pi,\pi]$ close to zero obeys

$$f(\omega) \sim C_2 |\omega|^{-2H+1}, \quad \text{as } \omega \to 0,$$

for $C_2 > 0$ and $1/2 < H < 1$.

If the logarithmic volatility component h_t exhibits long-range dependence properties, it leads to the formulation of the long memory stochastic volatility model (LMSV), pioneered by Harvey (1998) and Breidt et al. (1998).

Traditionally, incorporating long-range dependence into stochastic volatility (SV) models involves modeling the latent log variance dynamics using an autoregressive fractionally integrated moving average (ARFIMA) process. In its simplest manifestation, the log variance h_t follows an ARFIMA(0,d,0) process, represented as:

$$r_t = \exp(h_t/2)\varepsilon_t, \quad \varepsilon_t \sim N(0,1), \tag{18}$$

$$(1-B)^d h_t = \eta_t, \quad \eta_t \sim N(0,\tau_\eta^{-1}), \tag{19}$$

In this context, the backshift operator B is employed, and the parameter $d \in (-0.5, 0.5)$ determines the fractional integration order.

Our approach here diverges from the traditional ARFIMA framework by introducing long-range dependence through a fractional Gaussian noise (fGn) process instead. Conceptually, an ARFIMA process arises from the fractional differencing of a discrete autoregressive moving average (ARMA) process, while an fGn originates from the fractional differentiation of a continuous Brownian motion (Hosking, 1981). Although closely related, particularly when the autoregressive and moving average orders of the ARFIMA process are both 0, there are notable distinctions between the two. The relationship between the Hurst exponent H and the fractional integration order d is given by $H = d + 0.5$.

The fractional Gaussian noise is defined by its autocorrelation function

$$\gamma(h) = \frac{1}{2}(|h+1|^{2H} - 2|h|^{2H} + |h-1|^{2H}), \quad h = 0,\ldots,n-1, \tag{20}$$

where $H \in (0,1)$ is the Hurst exponent (or self-similarity parameter) and τ denotes the marginal precision parameter. Note that the fGn reduces to uncorrelated white noise when $H = 0.5$. If $H > 0.5$ the process has positive correlation, and, similarly, if $H < 0.5$, the autocorrelation is negative. In this work we allow each latent factor to have a distinct H parameter.

Another representation of the fGn process can be made by the definition of the fGn as the difference of a fractional Brownian Motion (e.g. Shi et al., 2022). Using the definition of a fractional Brownian motion (Mandelbrot and Van Ness, 1968):

$$B_{H_t} = \frac{1}{\Gamma(H+0.5)} \int_{-\infty}^{t} (t-s)^{H-0.5} - (-s)^{H-0.5} dB(s) + \int_{0}^{t} (t-s)^{H-0.5} dB(s) \tag{21}$$

B_{H_t} is the fractional Brownian motion process with Hurst parameter H, $dB(s)$ is the standard Brownian motion, and $\Gamma()$ is the gamma function. Using y_t as the trajectory of the process, the fGn can be defined as:

$$y_t = \sigma \left(B_{H_t} - B_{H_{1t-1}} \right) \tag{22}$$

with σ being the standard deviation of the process.

2.3 Gaussian Markov Random Field approximation of Fractional Gaussian Noise

Sørbye et al. (2017) leverage the established connection between long memory and cross-sectional aggregation (Granger, 1980; Beran et al., 2010) to devise a Gaussian Markov Random Field (GMRF) approximation for a fractional Gaussian noise (fGn) model. Their method involves constructing the approximation using weighted sums of independent autoregressive (AR(1)) components. The goal is to align the autocorrelation function of this composite autoregressive process with the autocorrelation function of an fGn processes.

Following Sørbye et al. (2017), consider m independent AR(1) processes

$$z_{j,t} = \phi_j z_{t-1} + \xi_{j,t}, \quad j = 1, \cdots, m, \quad t = 1, \cdots, n,$$

where $0 < \phi_j < 1$ represents the first-order autoregressive parameter of the j-th process. Additionally, let $\xi_{j,t} j = 1^m$ denote zero-mean independent Gaussian shocks with variance $\sigma^2 \xi, j = 1 - \phi_j^2$. The cross-sectional aggregation of the m processes is then defined as:

$$\bar{z}_m = \sigma \sum_{j=1}^{m} \sqrt{w_j z^{(j)}}, \tag{23}$$

Here, $z^{(j)}$ denotes $(z_{j,1}, z_{j,2}, \ldots, z_{j,n})$, and the weights w_j sum to one. Haldrup and Valdés (2017) investigate the finite sample properties of analogous aggregations of AR(1) processes.

The autocorrelation function of (23) is

$$\gamma_{\bar{z}_m}(k) = \sum_{j=1}^{m} w_j \phi_j^{|k|}, \quad k = 0,1,\ldots,n-1. \tag{24}$$

The proposal by Sørbye et al. (2017) involves determining weights $\boldsymbol{w} = {w_j}_{j=1}^{m}$ and coefficients $\boldsymbol{\phi} = {\phi_j}_{j=1}^{m}$ such that the autocorrelation function of the composite AR(1) process aligns with the autocorrelation function of a genuine fGn process. The values of $(\boldsymbol{w}, \boldsymbol{\phi})$ are obtained by minimizing the squared error

$$(\boldsymbol{w}, \boldsymbol{\phi})_H = \underset{(\boldsymbol{w},\boldsymbol{\phi})}{\operatorname{argmin}} \sum_{k=1}^{k_{\max}} \frac{1}{k} \left(\gamma_{\bar{z}_m}(k) - \gamma_{fGn}(k)\right)^2, \tag{25}$$

where k_{max} represents an arbitrary upper limit to the number of lags included. Since the squared error is weighted by k, persistence at distant lags has little impact on the objective function (25).

With this approximation of the fGn process, we can represent the fGn latent factor as a latent GMRF and estimate it using the INLA method, as demonstrated by Martino et al. (2011). Following the recommendations in Sørbye et al. (2017), we employ a third-order approximation to represent the fGn process. Further implementation details can be found in Sørbye et al. (2017). Using this structure the latent factor using this structure is denoted by:

$$h_t = fGn(H, 1/\tau_{fGn}) \tag{26}$$

We assume penalized complexity priors for the parameter H and the precision τ_{fGn}. See (Simpson et al., 2017) for a discussion on the use of this priors structure.

3. Dataset

We analyze the daily returns of five cryptocurrencies: Bitcoin (BTC), Etherium (ETH), Ripple (XRP), Solana (SOL) and Binance Coin (BNB) for the period from 2020-04-11 to 2023-11-18, representing a sample containing 1316 observations for each asset. Figure 1 presents the returns on these assets.

Figure 1
Daily Returns - Bitcoin (BTC), Etherium (ETH), Ripple (XRP), Solana (SOL) and Binance Coin (BNB)

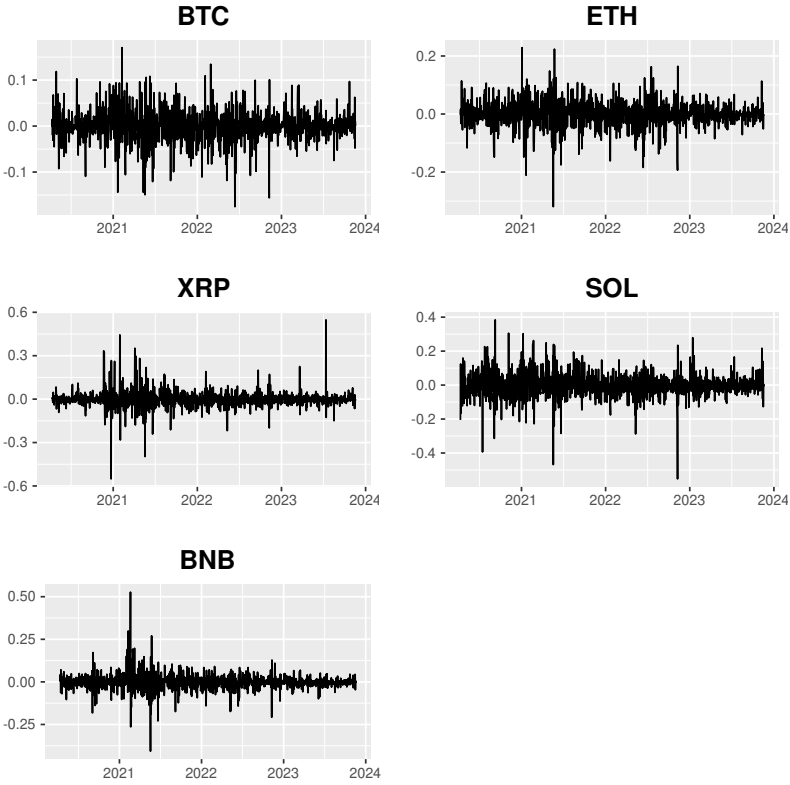

Descriptive statistics are presented in Table 1. We can observe that all

cryptocurrencies present positive returns in the period under analysis, but they are characterized by high standard deviations, very extreme values at maximum and minimum and high kurtosis, consistent with stylized facts of financial series, and the patterns of asymmetry and extreme returns are consistent with the dynamics observed in the cryptocurrency market, as discussed in Chaim and Laurini (2018) and Vieira and Laurini (2023).

Table 1
Descriptive Statistics

	Mean	Median	Sd	Skewness	Kurtosis	Min	Max	JB p-value
BTC	0.00127	0.00061	0.03320	-0.18017	6.55222	-0.17405	0.17182	0.00000
ETH	0.00191	0.00154	0.04372	-0.39731	7.96302	-0.31746	0.23070	0.00000
XRP	0.00089	0.00052	0.05859	0.69508	23.18818	-0.55050	0.54855	0.00000
SOL	0.00312	-0.00030	0.07298	-0.28029	9.24080	-0.54958	0.38718	0.00000
BNB	0.00219	0.00135	0.04808	0.73855	22.18095	-0.40445	0.52922	0.00000

4. Results

To analyze the impact of the model structure on the fit of the observed cryptocurrency series, we estimated all possible combinations of models with one to four latent factors, with all possible combinations of structures for the latent factors, representing a universe of 70 possible models. We present below comparisons between models using an information criterion (WAIC), adjustment measures (Root Mean Square Error and Mean Absolute Error) in-sample and out-of-sample, as well as the construction of a model confidence set with the set of the best models in terms of predictive performance.

4.1 Model Comparison using WAIC

As a preliminary assessment of model performance for the considered assets we compare in sample fit using an information criterion, which allows us to choose models with a good adjustment metric while penalizing more complex models. To perform this analysis we calculated for all Watanabe–Akaike information criterion (WAIC) models, introduced by Watanabe (2010). The WAIC is a generalized version of the Akaike information criterion (AIC) for models estimated using Bayesian procedures.

We present the results of the comparison of the estimated models using WAIC in Table 2. The Table shows an ordered list of the best models in terms of WAIC, with WAIC being interpreted in the usual way of information criteria where a lower value indicates a better tradeoff between adjustment and model complexity.

Results from 2 suggest the best model as chosen via WAIC has four common factors, three of which follow AR(1) processes and one following a RW2

process. The second best model is also composed by four factors, three following AR(1) processes and one whose dynamics are given by a RW1 process.

We thus find evidence of adjustment gains to be obtained by including a factor able to capture low frequency variations in the level of volatility within the cryptocurrency sector, represented by an RW2 process that assumes that this change in level occurs smoothly, or an RW1 process which assumes that permanent variations in the level of volatility follow a non-differentiable random process.

The presence of permanent changes in the level of cryptocurrency volatility is already a established stylized fact that has been extensively studied in this market, and modeled in various alternative ways using, for example, jump structures in the conditional variance (Chaim and Laurini, 2018, 2019b), Integrated GARCH models (Øverland Bergsli, Lind, Molnár and Polasik, 2022), structural breaks in the conditional variance (Aharon et al., 2023), and regime changes (Ardia et al., 2019). Furthermore, the existence of a permanent and smooth variation component in the level of cryptocurrencies has already been observed by Chevallier and Sanhaji (2023), who introduce a smoothly varying permanent component in the level of latent volatility for Bitcoin and Ethereum, this is an alternative specification based in the model of Engle and Rangel (2008) model, which is employed in order to capture this effect.

It is also important to note that the original formulation of the multifactor model with AR(1) dynamics for the latent factors proposed by Nacinben and Laurini (2024) is only the fourth best model according to the WAIC criterion, which indicates that the introduction of alternative dynamics for the latent factors represents potential gains in adjustment in relation to the usual factor dynamics that assume autoregressive processes with mean reversion.

We present in Table 3 the posterior distribution of the estimated parameters for the best model selected by WAIC - Four factor model with (AR(1), AR(1), AR(1), RW2) factor dynamics, and in Figure 2 graphs with posterior mean and 95% credibility intervals for the estimated latent factors. We can observe that the RW2 factor captures the smooth change in the level of conditional variance, which is transmitted to each series by the loadings associated with this factor. We can also observe that two AR(1) factors have a higher persistence (persistence parameters with a subsequent average of 0.964 and 0.922), and one factor with low persistence, with an average for the persistence parameter with a value of 0.209. It is also interesting to note that the AR(1) factor associated with lower persistence presents the greatest variability, and in this aspect captures shocks of greater amplitude and lower persistence in the conditional variance.

Table 2
Watanabe–Akaike information criterion (WAIC) Model Comparison

Rank	Model	F1	F2	F3	F4	WAIC
1	39	AR(1)	AR(1)	AR(1)	RW2	-26400.68
2	38	AR(1)	AR(1)	AR(1)	RW1	-26399.85
3	62	fGn	RW1	RW1	RW1	-26399.39
4	36	AR(1)	AR(1)	AR(1)	AR(1)	-26394.38
5	64	fGn	RW1	RW2	RW2	-26391.41
6	44	AR(1)	AR(1)	RW1	RW2	-26378.73
7	37	AR(1)	AR(1)	AR(1)	fGn	-26375.02
8	59	fGn	fGn	RW1	RW1	-26370.86
9	53	AR(1)	RW1	RW1	RW2	-26369.98
10	45	AR(1)	AR(1)	RW2	RW2	-26367.62
11	63	fGn	RW1	RW1	RW2	-26367.13
12	17	∅	AR(1)	AR(1)	fGn	-26366.90
13	49	AR(1)	fGn	RW1	RW1	-26365.78
14	60	fGn	fGn	RW1	RW2	-26365.58
15	41	AR(1)	AR(1)	fGn	RW1	-26362.82
16	21	∅	AR(1)	fGn	RW1	-26360.68
17	54	AR(1)	RW1	RW2	RW2	-26360.33
18	65	fGn	RW2	RW2	RW2	-26356.99
19	61	fGn	fGn	RW2	RW2	-26355.14
20	42	AR(1)	AR(1)	fGn	RW2	-26352.81
21	22	∅	AR(1)	fGn	RW2	-26352.44
22	50	AR(1)	fGn	RW1	RW2	-26351.77
23	57	fGn	fGn	fGn	RW1	-26347.00
24	20	∅	AR(1)	fGn	fGn	-26344.61
25	40	AR(1)	AR(1)	fGn	fGn	-26344.35
26	58	fGn	fGn	fGn	RW2	-26340.00
27	47	AR(1)	fGn	fGn	RW1	-26337.53
28	27	∅	fGn	fGn	RW1	-26335.43
29	51	AR(1)	fGn	RW2	RW2	-26335.06
30	56	fGn	fGn	fGn	fGn	-26320.85
31	46	AR(1)	fGn	fGn	fGn	-26308.11
32	26	∅	fGn	fGn	fGn	-26303.52
33	28	∅	fGn	fGn	RW2	-26278.69
34	16	∅	AR(1)	AR(1)	AR(1)	-26273.55
35	18	∅	AR(1)	AR(1)	RW1	-26269.93
36	19	∅	AR(1)	AR(1)	RW2	-26267.09
37	48	AR(1)	fGn	fGn	RW2	-26259.46
38	7	∅	∅	AR(1)	fGn	-26229.10
39	52	AR(1)	RW1	RW1	RW1	-26213.94
40	11	∅	∅	fGn	RW1	-26213.01
41	66	RW1	RW1	RW1	RW1	-26196.20
42	67	RW1	RW1	RW1	RW2	-26195.81
43	12	∅	∅	fGn	RW2	-26195.68
44	6	∅	∅	AR(1)	AR(1)	-26195.68
45	68	RW1	RW1	RW2	RW2	-26175.66
46	10	∅	∅	fGn	fGn	-26159.52
47	23	∅	AR(1)	RW1	RW1	-26142.42
48	32	∅	RW1	RW1	RW1	-26136.99
49	69	RW1	RW2	RW2	RW2	-26130.30
50	24	∅	AR(1)	RW1	RW2	-26123.44
51	29	∅	fGn	RW1	RW1	-26120.01
52	30	∅	fGn	RW1	RW2	-26101.85
53	33	∅	RW1	RW1	RW2	-26072.15
54	8	∅	∅	AR(1)	RW1	-26048.03
55	9	∅	∅	AR(1)	RW2	-26033.61
56	43	AR(1)	AR(1)	RW1	RW1	-26016.41
57	13	∅	∅	RW1	RW1	-25999.18
58	3	∅	∅	∅	fGn	-25976.32
59	14	∅	∅	RW1	RW2	-25954.10
60	2	∅	∅	∅	AR(1)	-25935.26
61	4	∅	∅	∅	RW1	-25761.16
62	70	RW2	RW2	RW2	RW2	-25407.07
63	34	∅	RW1	RW2	RW2	-25351.96
64	35	∅	RW2	RW2	RW2	-25342.14
65	31	∅	fGn	RW2	RW2	-25307.14
66	15	∅	∅	RW2	RW2	-25036.13
67	5	∅	∅	∅	RW2	-25008.42
68	55	AR(1)	RW2	RW2	RW2	-24926.85
69	25	∅	AR(1)	RW2	RW2	-24915.28
70	1	∅	∅	∅	∅	-20912.77

Note: F1, F2, F3 and F4 denote the stochastic process assumed for the latent factors. ∅ - Factor not included, AR(1) - First order autoregressive process,

RW1 - First order random walk, RW2 - Second-order random walk, fGn - fractional Gaussian noise.

Table 3
Posterior Distribution of Estimated Parameters - Model 39 - Four factor model with (AR(1),AR(1),AR(1),RW2) factor dynamics

	mean	sd	0.025quant	0.5quant	0.975quant	mode
μ_1	-7.765	0.043	-7.849	-7.765	-7.681	-7.765
μ_2	-7.162	0.042	-7.245	-7.162	-7.080	-7.162
μ_3	-6.988	0.044	-7.074	-6.988	-6.903	-6.988
μ_4	-5.898	0.042	-5.981	-5.898	-5.815	-5.898
μ_5	-7.222	0.043	-7.306	-7.222	-7.138	-7.222
τ_1	135509.597	104779.739	30620.580	106848.255	414205.361	68879.478
τ_2	2.429	0.237	1.993	2.418	2.926	2.398
ϕ_2	0.209	0.055	0.101	0.209	0.316	0.208
τ_3	27.418	16.521	8.204	23.406	70.542	17.259
ϕ_3	0.964	0.012	0.935	0.966	0.983	0.969
τ_4	36.533	17.327	13.943	32.916	80.447	26.812
ϕ_2	0.922	0.054	0.778	0.937	0.983	0.959
$\gamma_{2,1}$	1.030	0.098	0.830	1.032	1.216	1.042
$\gamma_{3,1}$	0.917	0.577	-0.225	0.919	2.048	0.926
$\gamma_{4,1}$	0.441	0.459	-0.460	0.441	1.347	0.437
$\gamma_{5,1}$	1.021	0.242	0.542	1.022	1.496	1.024
$\gamma_{2,2}$	1.764	0.136	1.497	1.764	2.031	1.764
$\gamma_{3,2}$	1.813	0.108	1.603	1.812	2.029	1.808
$\gamma_{4,2}$	1.269	0.159	0.957	1.269	1.582	1.269
$\gamma_{5,2}$	1.638	0.141	1.358	1.639	1.914	1.642
$\gamma_{2,3}$	1.115	0.379	0.378	1.112	1.870	1.099
$\gamma_{3,3}$	1.656	0.985	-0.259	1.648	3.619	1.614
$\gamma_{4,3}$	3.151	0.697	1.818	3.138	4.560	3.082
$\gamma_{5,3}$	2.931	0.492	1.976	2.926	3.912	2.907
$\gamma_{2,4}$	1.249	0.481	0.296	1.251	2.188	1.260
$\gamma_{3,4}$	-3.349	0.669	-4.688	-3.341	-2.053	-3.311
$\gamma_{4,4}$	1.294	0.773	-0.206	1.286	2.838	1.254
$\gamma_{5,4}$	0.308	0.523	-0.704	0.302	1.356	0.277

Note: μ_i denotes the mean for the latent factor i. τ_i is the precision for the latent factor i. ϕ_i is the autoregressive parameters in the case of an AR(1) factor. $\gamma_{j,k}$ is the factor loading for the factor k in the series j.

4.2 In-sample Fit Measures

The results of the analysis using WAIC indicate which is the best model in terms of a tradeoff between posterior likelihood and model complexity. An alternative fit analysis can be performed using model fit measures, comparing the conditional volatilities measured by the model against some proxy for the true unobserved volatilide. To carry out these analyzes we present in Tables 4 and 5 the root mean squared error (RMSE) and the mean absolute error (MAE) between the conditional volatilities adjusted by all the models analyzed for the set of cryptocurrencies under analysis. In these an-

Figure 2
Latent Factors - Model 39 - Four factor model with (AR(1),AR(1),AR(1),RW2) factor dynamics

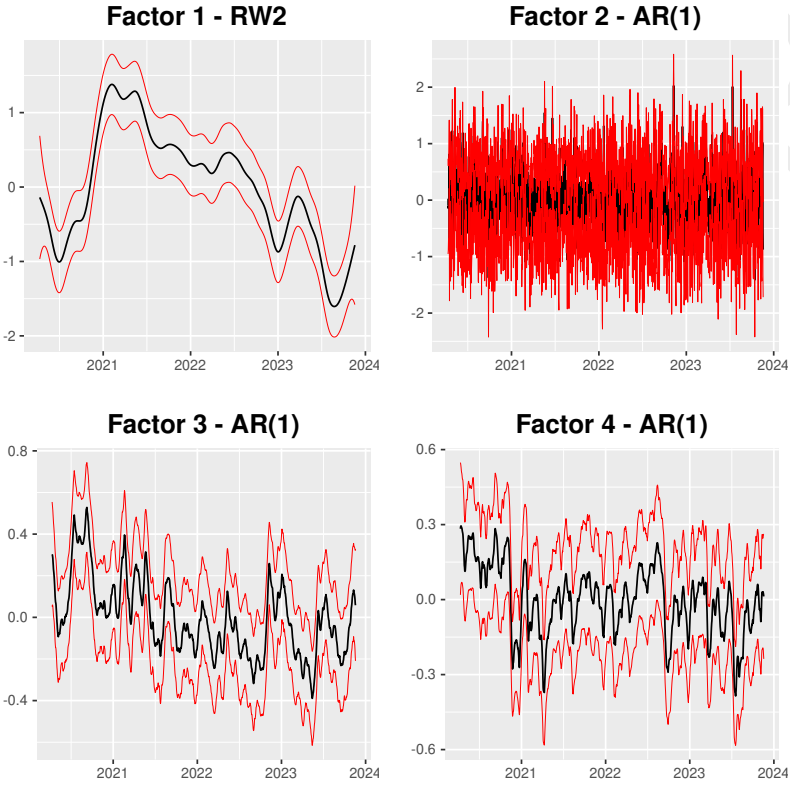

alyzes we use the absolute returns of each asset as a proxy for unobserved conditional volatility. Note that both RMSE and MAE can be viewed as loss metrics when we consider quadratic and absolute loss functions, respectively (Robert, 2001).

In Tables 4 and 5 the best value for each asset is denoted in bold. Regarding RMSE, the best model for BTC is model 58, which is a model with four

factors and dynamics (fGn, fGn, fGn, RW2), for ETH the best model is model 37 with four factors and dynamics (AR(1), AR(1), AR(1), fGn), and for the XRP, SOL and BNB series the best model in terms of RMSE is model 10 with only two factors and dynamics (fGn, fGn). These results indicate that in terms of adjustment by the Root Mean Square Error metric, latent factors with long memory dynamics seem to indicate adjustment gains for most series.

For the MAE metric the results are similar. The best model for the XRP, SOL and BNB series is also model 10 with just two factors and dynamics (fGn, fGn), for ETH the best model again is model 37 with four factors and dynamics (AR(1), AR(1), AR(1), fGn) and BTC the best model is 57, with four factors and dynamics (fGn, fGn, fGn, RW1). These results again indicate that the use of latent factors with long memory is relevant for the predictive gain, and that for the BTC series processes RW1 and RW2 are important for the in-sample adjustment.

We can also observe that the composition of more than one factor with RW1 RW2 dynamics can lead to adjustment problems in the model, as can be observed by the high values in the RMSE and MAE metrics for models with these characteristics, which may indicate identification problems.

We show in Table 6 the posterior distribution of the estimated parameters for model 10, which was the model with the best fit in terms of RMSE and MAE for the XRP, SOL and BNB series, and in Figure 3 graphs with posterior mean and 95% credibility intervals for the two estimated fGn latent factors. The model presents H parameters with posterior averages of 0.812 and 0.798, compatible with the presence of long memory in this dynamic structure. It is also interesting to note that the first factor fGn captures the change in the level of variance that occurred close to the year 2021.

Figure 3
Latent Factors - Model 39 - Two factor model with (fGn,fGn) factor dynamics

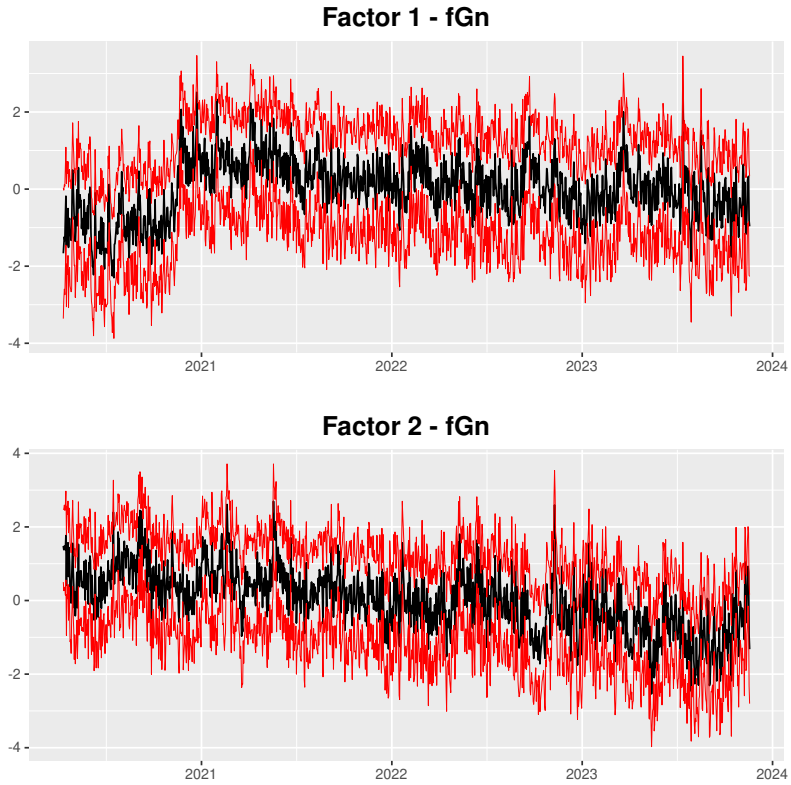

Table 4
In-sample Root Mean Squared Error

	Model	BTC	ETH	XRP	SOL	BNB
1	∅ ∅ ∅ ∅	0.02646	0.03415	0.05308	0.05682	0.04190
2	∅ ∅ ∅ AR(1)	0.01795	0.02137	0.03162	0.04215	0.02344
3	∅ ∅ ∅ fGn	0.01799	0.02134	0.03166	0.04220	0.02321
4	∅ ∅ ∅ RW1	0.01908	0.02280	0.03292	0.04281	0.02404
5	∅ ∅ ∅ RW2	0.02188	0.02664	0.03772	0.04582	0.02840
6	∅ ∅ AR(1) AR(1)	0.01702	0.02118	0.02813	0.09080	0.03420
7	∅ ∅ AR(1) fGn	0.01720	0.02034	0.04773	0.18328	0.02262
8	∅ ∅ AR(1) RW1	0.01654	0.02344	0.02994	0.04465	0.02802
9	∅ ∅ AR(1) RW2	0.01697	0.02335	0.03008	0.04404	0.02680
10	∅ ∅ fGn fGn	0.01716	0.02032	**0.02317**	**0.03662**	**0.02151**
11	∅ ∅ fGn RW1	0.01756	0.02083	0.02934	0.05635	0.02365
12	∅ ∅ fGn RW2	0.01780	0.02098	0.03033	0.04512	0.02322
13	∅ ∅ RW1 RW1	0.01878	0.02217	0.03091	0.05391	0.02390
14	∅ ∅ RW1 RW2	0.01909	0.02242	0.03285	0.04419	0.02445
15	∅ ∅ RW2 RW2	0.02220	0.02816	0.03962	0.04801	0.03158
16	∅ AR(1) AR(1) AR(1)	0.01595	0.04142	0.08048	0.15591	0.03988
17	∅ AR(1) AR(1) fGn	0.01509	0.01866	0.03870	0.09892	0.02813
18	∅ AR(1) AR(1) RW1	0.01617	0.04403	0.09135	0.10233	0.04008
19	∅ AR(1) AR(1) RW2	0.01649	0.04970	0.09894	0.11512	0.04451
20	∅ AR(1) fGn fGn	0.01482	0.06470	0.20624	0.07449	0.10548
21	∅ AR(1) fGn RW1	0.01512	0.08531	0.77117	1.80579	0.16267
22	∅ AR(1) fGn RW2	0.01519	0.07626	0.57859	0.08074	0.08478
23	∅ AR(1) RW1 RW1	0.01685	0.08728	2.55173	0.11264	0.12005
24	∅ AR(1) RW1 RW2	0.01724	0.10861	2.07056	0.04445	0.14980
25	∅ AR(1) RW2 RW2	0.02227	4.22490	757.269	0.23356	25.32719
26	∅ fGn fGn fGn	0.01458	0.06180	0.11197	0.07767	0.06715
27	∅ fGn fGn RW1	0.01512	0.08904	0.11897	0.06459	0.07243
28	∅ fGn fGn RW2	0.01572	0.05605	0.07947	0.04409	0.04561
29	∅ fGn RW1 RW1	0.01690	0.06567	0.26731	0.050920	0.09738
30	∅ fGn RW1 RW2	0.01710	0.10053	0.19772	0.043801	0.11100
31	∅ fGn RW2 RW2	0.02408	1.14274	0.09183	0.86557	1.11398
32	∅ RW1 RW1 RW1	0.01700	0.09116	0.71802	0.55629	0.16727
33	∅ RW1 RW1 RW2	0.01729	0.99375	0.40813	0.23093	0.99169
34	∅ RW1 RW2 RW2	0.02048	282.57549	417.52604	4.25040	2842.51362
35	∅ RW2 RW2 RW2	0.02120	1.86628	12.77634	0.17893	6.98277
36	AR(1) AR(1) AR(1) AR(1)	0.01444	0.03563	1.44507	0.11555	0.06733
37	AR(1) AR(1) AR(1) fGn	0.01508	**0.01849**	0.04356	0.10973	0.02842
38	AR(1) AR(1) AR(1) RW1	0.01444	0.03509	0.10923	0.07303	0.04577
39	AR(1) AR(1) AR(1) RW2	0.01442	0.03585	0.10219	0.13374	0.08030
40	AR(1) AR(1) fGn fGn	0.01490	0.06347	0.17876	0.06043	0.07709
41	AR(1) AR(1) fGn RW1	0.01502	0.02680	0.18521	0.21362	0.09688
42	AR(1) AR(1) fGn RW2	0.01512	0.08382	0.47860	0.07326	0.09231
43	AR(1) AR(1) RW1 RW1	0.01791	0.11726	0.14129	0.08082	0.20531
44	AR(1) AR(1) RW1 RW2	0.01474	0.08087	0.39307	0.06250	0.19753
45	AR(1) AR(1) RW2 RW2	0.01483	0.15649	0.12408	1.98395	0.63291
46	AR(1) fGn fGn fGn	0.01469	0.06496	0.11722	0.13280	0.07368
47	AR(1) fGn fGn RW1	0.01502	0.08921	0.12844	0.06704	0.07691
48	AR(1) fGn fGn RW2	0.01667	0.04535	0.12707	0.05104	0.03869
49	AR(1) fGn RW1 RW1	0.01490	0.03019	0.43110	0.05088	0.06246
50	AR(1) fGn RW1 RW2	0.01454	0.03682	0.10083	0.57192	0.20498
51	AR(1) fGn RW2 RW2	0.01464	0.16468	0.05022	2.54997	0.82022
52	AR(1) RW1 RW1 RW1	0.01615	0.04234	0.08460	0.18258	0.09699
53	AR(1) RW1 RW1 RW2	0.01526	0.03035	0.15736	0.05503	0.03048
54	AR(1) RW1 RW2 RW2	0.01520	0.20011	0.26977	0.10239	0.48283
55	AR(1) RW2 RW2 RW2	0.02150	433.64499	2325.71063	4.02178	53392.59409
56	fGn fGn fGn fGn	0.01442	0.04556	0.05654	0.04604	0.03933
57	fGn fGn fGn RW1	0.01439	0.04503	0.23364	0.04782	0.04164
58	fGn fGn fGn RW2	**0.01433**	0.03215	0.07359	0.04404	0.03055
59	fGn fGn RW1 RW1	0.01447	0.02409	0.05639	0.26838	0.07461
60	fGn fGn RW1 RW2	0.01449	0.02560	0.04326	0.08043	0.02817
61	fGn fGn RW2 RW2	0.01477	0.32366	0.03132	6.80948	4.01551
62	fGn RW1 RW1 RW1	0.01509	0.02636	0.93554	0.09866	0.05898
63	fGn RW1 RW1 RW2	0.01596	0.02611	0.07138	0.04490	0.07484
64	fGn RW1 RW2 RW2	0.01559	0.04468	0.24135	0.04728	0.03311
65	fGn RW2 RW2 RW2	0.01592	0.28916	0.03539	0.04680	0.12728
66	RW1 RW1 RW1 RW1	0.01676	0.10706	0.61435	0.45242	0.58722
67	RW1 RW1 RW1 RW2	0.01673	0.36123	0.36916	0.29672	0.48977
68	RW1 RW1 RW2 RW2	0.01711	0.81411	0.87652	3.24925	5.35631
69	RW1 RW2 RW2 RW2	0.01746	1.57466	0.06531	0.59166	3.19248
70	RW2 RW2 RW2 RW2	0.02071	0.09223	0.18822	0.08573	0.15521

Note: ∅ - Factor not included, AR(1) - First order autoregressive process, RW1 - First order random walk, RW2 - Second-order random walk, fGn - fractional Gaussian noise. Numerical convergence of the estimator displayed problems for particular combinations of factor specification and samples, in these cases we do not present the fit measures.

Table 5
In-sample Mean Absolute Error

	Model	BTC	ETH	XRP	SOL	BNB
1	∅ ∅ ∅ ∅	0.02212	0.02786	0.04092	0.04590	0.03259
2	∅ ∅ ∅ AR(1)	0.01211	0.01444	0.01891	0.03027	0.01457
3	∅ ∅ ∅ fGn	0.01213	0.01432	0.01890	0.03021	0.01440
4	∅ ∅ ∅ RW1	0.01315	0.01554	0.01990	0.03103	0.01528
5	∅ ∅ ∅ RW2	0.01595	0.01913	0.02397	0.03409	0.01863
6	∅ ∅ AR(1) AR(1)	0.01126	0.01444	0.01731	0.06479	0.02125
7	∅ ∅ AR(1) fGn	0.01166	0.01380	0.02792	0.07863	0.01456
8	∅ ∅ AR(1) RW1	0.01113	0.01555	0.01805	0.03184	0.01856
9	∅ ∅ AR(1) RW2	0.01137	0.01550	0.01816	0.03136	0.01759
10	∅ ∅ fGn fGn	0.01164	0.01370	**0.01517**	**0.02609**	**0.01388**
11	∅ ∅ fGn RW1	0.01162	0.01403	0.01811	0.04171	0.01450
12	∅ ∅ fGn RW2	0.01166	0.01410	0.01802	0.03188	0.01441
13	∅ ∅ RW1 RW1	0.01277	0.01522	0.02012	0.03959	0.01514
14	∅ ∅ RW1 RW2	0.01294	0.01532	0.01980	0.03118	0.01565
15	∅ ∅ RW2 RW2	0.01647	0.02025	0.02590	0.03497	0.02083
16	∅ AR(1) AR(1) AR(1)	0.01076	0.01941	0.03478	0.06630	0.02090
17	∅ AR(1) AR(1) fGn	0.01039	0.01315	0.02207	0.05224	0.01787
18	∅ AR(1) AR(1) RW1	0.01084	0.02019	0.03508	0.04866	0.02080
19	∅ AR(1) AR(1) RW2	0.01093	0.02178	0.03596	0.05154	0.02209
20	∅ AR(1) fGn fGn	0.01020	0.02671	0.06117	0.04127	0.03727
21	∅ AR(1) fGn RW1	0.01038	0.03115	0.17300	0.49397	0.05619
22	∅ AR(1) fGn RW2	0.01040	0.02897	0.13925	0.04501	0.03301
23	∅ AR(1) RW1 RW1	0.01181	0.03289	0.41204	0.07745	0.04362
24	∅ AR(1) RW1 RW2	0.01206	0.04351	0.36967	0.03109	0.05100
25	∅ AR(1) RW2 RW2	0.01676	1.05423	110.73542	0.1288	4.89848
26	∅ fGn fGn fGn	0.01009	0.02582	0.04035	0.04289	0.02759
27	∅ fGn fGn RW1	0.01043	0.03215	0.04287	0.04802	0.03073
28	∅ fGn fGn RW2	0.01045	0.02522	0.03459	0.02938	0.02219
29	∅ fGn RW1 RW1	0.01180	0.02923	0.08428	0.03219	0.03565
30	∅ fGn RW1 RW2	0.01197	0.04207	0.09546	0.03077	0.04127
31	∅ fGn RW2 RW2	0.01917	0.35900	0.03366	0.29736	0.30688
32	∅ RW1 RW1 RW1	0.01185	0.03424	0.17763	0.174114	0.05457
33	∅ RW1 RW1 RW2	0.01193	0.23766	0.12614	0.09790	0.25464
34	∅ RW1 RW2 RW2	0.01498	44.37092	58.90639	1.09543	374.22625
35	∅ RW2 RW2 RW2	0.01523	0.44959	2.34124	0.09000	1.34413
36	AR(1) AR(1) AR(1) AR(1)	0.00999	0.01803	0.28625	0.06783	0.02893
37	AR(1) AR(1) AR(1) fGn	0.01034	**0.01300**	0.02578	0.05568	0.01807
38	AR(1) AR(1) AR(1) RW1	0.00998	0.01796	0.04031	0.03908	0.02197
39	AR(1) AR(1) AR(1) RW2	0.00995	0.01792	0.05062	0.05873	0.03274
40	AR(1) AR(1) fGn fGn	0.01025	0.02641	0.05831	0.03637	0.03011
41	AR(1) AR(1) fGn RW1	0.01033	0.01527	0.06224	0.08824	0.03755
42	AR(1) AR(1) fGn RW2	0.01035	0.03123	0.12261	0.04213	0.03483
43	AR(1) AR(1) RW1 RW1	0.01268	0.04305	0.05393	0.03611	0.06388
44	AR(1) AR(1) RW1 RW2	0.01018	0.04021	0.10612	0.04070	0.07986
45	AR(1) AR(1) RW2 RW2	0.01022	0.06561	0.04894	0.64374	0.20224
46	AR(1) fGn fGn fGn	0.01014	0.02659	0.04119	0.06069	0.02944
47	AR(1) fGn fGn RW1	0.01039	0.03232	0.04482	0.04986	0.03185
48	AR(1) fGn fGn RW2	0.01120	0.02089	0.04326	0.03059	0.02019
49	AR(1) fGn RW1 RW1	0.01018	0.01938	0.14050	0.03312	0.03201
50	AR(1) fGn RW1 RW2	0.01005	0.02239	0.03765	0.17963	0.07175
51	AR(1) fGn RW2 RW2	0.01013	0.06880	0.02604	0.81536	0.25653
52	AR(1) RW1 RW1 RW1	0.01150	0.02443	0.03677	0.07536	0.03942
53	AR(1) RW1 RW1 RW2	0.01044	0.01878	0.06006	0.03659	0.01979
54	AR(1) RW1 RW2 RW2	0.01035	0.09284	0.08926	0.05846	0.18232
55	AR(1) RW2 RW2 RW2	0.01618	61.4890	277.96864	1.06184	5325.28730
56	fGn fGn fGn fGn	0.00992	0.02144	0.02589	0.03050	0.01998
57	fGn fGn fGn RW1	**0.00990**	0.02108	0.06119	0.03010	0.02108
58	fGn fGn fGn RW2	0.00991	0.01696	0.02938	0.02874	0.01737
59	fGn fGn RW1 RW1	0.00999	0.01555	0.02672	0.13560	0.03705
60	fGn fGn RW1 RW2	0.00999	0.01772	0.02515	0.04673	0.01807
61	fGn fGn RW2 RW2	0.01015	0.12683	0.02142	2.29727	1.25367
62	fGn RW1 RW1 RW1	0.01029	0.01679	0.27795	0.05575	0.03189
63	fGn RW1 RW1 RW2	0.01034	0.01880	0.03521	0.03110	0.03455
64	fGn RW1 RW2 RW2	0.01050	0.02699	0.08005	0.03347	0.02014
65	fGn RW2 RW2 RW2	0.01070	0.12382	0.02008	0.03308	0.06384
66	RW1 RW1 RW1 RW1	0.01166	0.03796	0.16378	0.15109	0.14478
67	RW1 RW1 RW1 RW2	0.01162	0.10273	0.11483	0.11704	0.13296
68	RW1 RW1 RW2 RW2	0.01187	0.26480	0.24991	1.03889	1.40366
69	RW1 RW2 RW2 RW2	0.01205	0.35441	0.03502	0.19665	0.68000
70	RW2 RW2 RW2 RW2	0.01503	0.04124	0.06969	0.05529	0.05994

Note: ∅ - Factor not included, AR(1) - First order autoregressive process, RW1 - First order random walk, RW2 - Second-order random walk, fGn - fractional Gaussian noise.

Table 6
Posterior Distribution of Estimated Parameters - Model 10 - Two factor model with (fGn,fGn) factor dynamics

	mean	sd	0.025quant	0.5quant	0.975quant	mode
μ_1	-7.684	0.043	-7.768	-7.684	-7.600	-7.684
μ_2	-7.126	0.042	-7.209	-7.126	-7.044	-7.126
μ_3	-6.966	0.045	-7.053	-6.966	-6.878	-6.966
μ_4	-5.901	0.043	-5.985	-5.901	-5.817	-5.901
μ_5	-7.230	0.043	-7.315	-7.230	-7.145	-7.230
τ_1	1.144	0.499	0.484	1.042	2.404	0.868
H_1	0.812	0.036	0.738	0.813	0.879	0.815
τ_2	1.099	0.469	0.453	1.010	2.265	0.853
H_2	0.798	0.050	0.693	0.801	0.886	0.810
$\gamma_{2,1}$	0.859	0.100	0.661	0.859	1.053	0.862
$\gamma_{3,1}$	1.344	0.174	1.008	1.342	1.691	1.335
$\gamma_{4,1}$	0.268	0.159	-0.055	0.271	0.571	0.286
$\gamma_{5,1}$	0.838	0.108	0.622	0.839	1.046	0.845
$\gamma_{2,2}$	1.068	0.058	0.955	1.067	1.184	1.064
$\gamma_{3,2}$	0.722	0.140	0.456	0.719	1.006	0.706
$\gamma_{4,2}$	1.055	0.139	0.782	1.055	1.330	1.054
$\gamma_{5,2}$	1.176	0.107	0.967	1.175	1.388	1.172

Note: μ_i denote the mean for the latent factor i. τ_i is the precision for the latent factor i. ϕ_i is the autoregressive parameters in the case of an AR(1) factor. $\gamma_{j,k}$ is the factor loading for the factor k in the series j.

5. Out-of-sample analysis

To verify the out-of-sample predictive performance, we performed an analysis comparing the predictions of all models for the last 30 observations in the sample. In this analysis, the last 30 observations in the sample are treated as unobserved values, and the models perform out-of-sample predictions treating the conditional volatilities in these observations as additional parameters to be estimated, as per the discussion in Nacinben and Laurini (2024). Thus our forecasting experiment can be considered as a 30-period forward dynamic forecast for conditional volatility.

We report in Tables 7 and 8 the forecast RMSE and MAE for all analysed models.

In this predictive analysis, the results are more diverse in relation to the choice of the best model. For the BTC series the best model both in terms of RMSE and MAE is model 19, which is a model with three factors (AR(1), AR(1), RW2), indicating the importance of the smooth change component in the level to predict BTC volatility in this period. For the ETH series, the best model by RMSE is model 43 (AR(1),AR(1),RW1 RW1) and by MAE model 54 (AR(1),RW1,RW2,RW2), indicating the need high persistence dynamics for forecasting this series in this sample. The same model 54 with four factors and dynamics (AR(1),RW1,RW2,RW2) is selected for the BNB series by the RMSE and MAE criteria, and for the SOL series the best model by both criteria is model 9, a two-factor model and dynamics (AR(1),RW2) for latent factors.

Although the results of choosing the best model in terms of predictive performance were more diverse, we can observe that again all models are composed of latent factors with dynamics distinct from the AR(1) process that is normally used in multivariate stochastic volatility models, indicating that the addition of factors with long memory, and first and second order random walks also represents gains in terms of out-of-sample predictive performance.

To complement the predictive performance analyses, we performed a complementary analysis by constructing the Model Confidence Set - MCS (Hansen et al., 2011) for each series analyzed, selecting the set of models with the best predictive performance, and sequentially eliminating the models with lower statistical performance, controlling for multiple comparisons and using bootstrap to construct tests with adequate power in finite samples and robustness to data snooping, as discussed in Hansen et al. (2011). We carried out the construction of the MCS using the squared error as a loss metric, 5.000 bootstrap replications and a significance level of 20%.

Tables 9-13 present the MCS selected for the five series. Details about the

reported test statistics can be found at Hansen et al. (2011). We can see that the MCS for the BTC series eliminates 61 models from the final set, containing 9 models in the final MCS, the MCS for ETH consists of 17 models, the MCS for XRP in a set of 8 models. For the SOL MCS series it eliminates only four models, and for the BNB series the reduction is only of three models.

Table 7
Out-of-sample Root Mean Squared Error

	Model	BTC	ETH	XRP	SOL	BNB
1	∅ ∅ ∅ ∅	0.02616	0.03416	0.04316	0.05170	0.03647
2	∅ ∅ ∅ AR(1)	0.03797	0.04798	0.05649	0.05769	0.05125
3	∅ ∅ ∅ fGn	0.02948	0.03659	0.03973	0.05204	0.03613
4	∅ ∅ ∅ RW1	0.77580	0.86074	1.40745	0.34632	1.42821
5	∅ ∅ ∅ RW2	1.06673	1.35582	3.65699	0.44273	3.87908
6	∅ ∅ AR(1) AR(1)	0.04280	0.05029	0.07423	0.06410	0.05391
7	∅ ∅ AR(1) fGn	0.03847	0.04809	0.06067	0.08084	0.05438
8	∅ ∅ AR(1) RW1	0.02397	0.02870	0.03054	0.04869	0.02442
9	∅ ∅ AR(1) RW2	0.02194	0.02455	0.02703	**0.04829**	0.01703
10	∅ ∅ fGn fGn	0.03604	0.03963	0.08194	0.05710	0.03803
11	∅ ∅ fGn RW1	0.03427	0.03734	0.08374	0.06547	0.03578
12	∅ ∅ fGn RW2	0.03538	0.03720	0.06045	0.05345	0.03329
13	∅ ∅ RW1 RW1	1.02772	0.90951	2.58249	0.18075	1.20964
14	∅ ∅ RW1 RW2	1.06025	0.94857	1.89675	0.21603	1.34475
15	∅ ∅ RW2 RW2	2.53872	7.20001	73.51091	0.48425	27.05859
16	∅ AR(1) AR(1) AR(1)	0.03217	0.05632	0.07629	0.06081	0.06962
17	∅ AR(1) AR(1) fGn	0.03671	0.04885	0.05185	0.08782	0.06126
18	∅ AR(1) AR(1) RW1	0.02168	0.02955	0.03161	0.05762	0.02478
19	∅ AR(1) AR(1) RW2	**0.02042**	0.02567	0.02751	0.06423	0.02031
20	∅ AR(1) fGn fGn	0.03422	0.08435	0.32656	0.07866	0.20569
21	∅ AR(1) fGn RW1	0.03279	0.08248	0.37830	0.07329	0.10951
22	∅ AR(1) fGn RW2	0.03794	0.10868	0.46452	0.12727	0.16929
23	∅ AR(1) RW1 RW1	1.63684	103.18791	141.99595	0.89684	114.57870
24	∅ AR(1) RW1 RW2	1.28412	146.97639	191.63105	2.58449	268.04849
25	∅ AR(1) RW2 RW2	0.18069	2.45132	0.34885	1.07997	4.97390
26	∅ fGn fGn fGn	0.03649	0.09614	0.17778	0.06215	0.09517
27	∅ fGn fGn RW1	0.03581	0.07154	0.25728	0.08483	0.07334
28	∅ fGn fGn RW2	0.02280	0.03883	0.04568	0.05046	0.02399
29	∅ fGn RW1 RW1	1.95203	189.05791	619.64457	3.34238	1155.16126
30	∅ fGn RW1 RW2	1.62040	150.72561	55.02334	2.12339	222.13178
31	∅ fGn RW2 RW2	0.18710	1.56059	0.09816	0.42812	1.03727
32	∅ RW1 RW1 RW1	1.49330	69.88340	206.82607	0.77638	94.40129
33	∅ RW1 RW1 RW2	0.85167	28.39485	58.86722	0.68852	23.64246
34	∅ RW1 RW2 RW2	30.92637	26382.50759	545941.24017	27.84709	325456.87161
35	∅ RW2 RW2 RW2	37.68718	21444.41200	225347.41538	25.89776	136766.97361
36	AR(1) AR(1) AR(1) AR(1)	0.02845	0.04598	0.68902	0.16664	0.10765
37	AR(1) AR(1) AR(1) fGn	0.03383	0.04325	0.04587	0.05055	0.04092
38	AR(1) AR(1) AR(1) RW1	0.02181	0.03204	0.08359	0.10985	0.06124
39	AR(1) AR(1) AR(1) RW2	0.02049	0.02781	0.02186	0.13023	0.04136
40	AR(1) AR(1) fGn fGn	0.03496	0.08859	0.61469	0.07286	0.15350
41	AR(1) AR(1) fGn RW1	0.03559	0.09590	0.69541	0.14092	0.28096
42	AR(1) AR(1) fGn RW2	0.03784	0.10742	0.51796	0.12979	0.15931
43	AR(1) AR(1) RW1 RW1	0.02081	**0.02261**	0.02255	0.06135	0.02729
44	AR(1) AR(1) RW1 RW2	0.02394	0.03157	0.12830	0.05202	0.03862
45	AR(1) AR(1) RW2 RW2	0.03066	0.04660	0.17100	0.17222	0.10055
46	AR(1) fGn fGn fGn	0.03840	0.10814	0.16744	0.06343	0.10554
47	AR(1) fGn fGn RW1	0.03679	0.07667	3.43478	0.06119	0.10493
48	AR(1) fGn fGn RW2	0.02321	0.03925	0.05080	0.05178	0.02466
49	AR(1) fGn RW1 RW1	0.02329	0.02837	**0.02177**	0.16378	0.05877
50	AR(1) fGn RW1 RW2	0.02586	0.06240	0.14800	0.16406	0.15111
51	AR(1) fGn RW2 RW2	0.02986	0.43054	0.10352	2.75097	1.57764
52	AR(1) RW1 RW1 RW1	0.02101	0.02288	0.15062	0.05729	0.02695
53	AR(1) RW1 RW1 RW2	0.02127	0.03103	0.06015	0.09098	0.04713
54	AR(1) RW1 RW2 RW2	0.02433	0.02487	0.03784	0.06031	**0.01493**
55	AR(1) RW2 RW2 RW2	0.02678	0.02513	0.02698	0.22100	0.04647
56	fGn fGn fGn fGn	0.04232	0.09607	0.23706	0.06704	0.07715
57	fGn fGn fGn RW1	0.03693	0.07766	0.97893	0.06562	0.05620
58	fGn fGn fGn RW2	0.02354	0.04135	0.07242	0.05751	0.04004
59	fGn fGn RW1 RW1	0.02407	0.02498	0.06277	0.05015	0.02514
60	fGn fGn RW1 RW2	0.02328	0.04283	0.05868	0.09128	0.03246
61	fGn fGn RW2 RW2	0.03618	2.23430	0.34841	220.53631	217.83405
62	fGn RW1 RW1 RW1	0.02406	0.02472	0.07653	0.09631	0.03752
63	fGn RW1 RW1 RW2	0.02339	0.02738	0.02862	0.06820	0.02214
64	fGn RW1 RW2 RW2	0.03053	0.02846	0.03127	0.05884	0.02068
65	fGn RW2 RW2 RW2	0.02062	0.03083	0.03884	48.82953	3.78482
66	RW1 RW1 RW1 RW1	1.83959	63.84841	701.74190	1.59187	7.65545
67	RW1 RW1 RW1 RW2	2.59832	35.22935	182.27478	1.87492	8.47454
68	RW1 RW1 RW2 RW2	1.28404	4263.94747	115961.54971	11.64143	7466.79268
69	RW1 RW2 RW2 RW2	2.74147	1.63616	2.42375	0.46951	0.99920
70	RW2 RW2 RW2 RW2	48.30088	4254.68418	181504.29077	27.57899	1507.66203

Note: ∅ - Factor not included, AR(1) - First order autoregressive process, RW1 - First order random walk, RW2 - Second-order random walk, fGn - fractional Gaussian noise.

Table 8
Out-of-sample Mean Absolute Error

	Model	BTC	ETH	XRP	SOL	BNB
1	∅ ∅ ∅ ∅	0.02361	0.03149	0.03949	0.04167	0.03353
2	∅ ∅ ∅ AR(1)	0.03576	0.04530	0.05208	0.04827	0.04905
3	∅ ∅ ∅ fGn	0.02706	0.03387	0.03562	0.04303	0.03333
4	∅ ∅ ∅ RW1	0.60397	0.67538	1.08155	0.29051	1.08885
5	∅ ∅ ∅ RW2	0.68808	0.87301	2.18170	0.32923	2.27379
6	∅ ∅ AR(1) AR(1)	0.04043	0.04762	0.07054	0.05555	0.05175
7	∅ ∅ AR(1) fGn	0.03574	0.04512	0.05580	0.07042	0.05105
8	∅ ∅ AR(1) RW1	0.02035	0.02480	0.02771	0.03988	0.02082
9	∅ ∅ AR(1) RW2	0.01719	0.01887	0.02434	**0.03833**	0.01413
10	∅ ∅ fGn fGn	0.03352	0.03681	0.07822	0.04805	0.03523
11	∅ ∅ fGn RW1	0.03182	0.03459	0.07991	0.05603	0.03297
12	∅ ∅ fGn RW2	0.03274	0.03443	0.05596	0.04413	0.03045
13	∅ ∅ RW1 RW1	0.78802	0.70645	1.94466	0.15190	0.91935
14	∅ ∅ RW1 RW2	0.80284	0.72803	1.43071	0.17885	1.00462
15	∅ ∅ RW2 RW2	1.41237	3.72441	33.20832	0.33127	12.66165
16	∅ AR(1) AR(1) AR(1)	0.02908	0.05265	0.06888	0.05158	0.06398
17	∅ AR(1) AR(1) fGn	0.03410	0.04580	0.04660	0.07546	0.05749
18	∅ AR(1) AR(1) RW1	0.01699	0.02619	0.02858	0.04874	0.02171
19	∅ AR(1) AR(1) RW2	**0.01429**	0.02132	0.02484	0.05442	0.01771
20	∅ AR(1) fGn fGn	0.03182	0.07785	0.29866	0.06846	0.19118
21	∅ AR(1) fGn RW1	0.03039	0.07596	0.35151	0.06178	0.10270
22	∅ AR(1) fGn RW2	0.03507	0.10027	0.43324	0.10292	0.15064
23	∅ AR(1) RW1 RW1	1.22415	66.68612	93.17879	0.68899	73.74407
24	∅ AR(1) RW1 RW2	0.97485	95.60664	128.54123	1.95352	171.20695
25	∅ AR(1) RW2 RW2	0.13400	1.30415	0.23648	0.66456	2.49712
26	∅ fGn fGn fGn	0.03397	0.08952	0.16996	0.05360	0.09016
27	∅ fGn fGn RW1	0.03321	0.06598	0.24321	0.07345	0.06934
28	∅ fGn fGn RW2	0.01863	0.03617	0.04068	0.04146	0.02157
29	∅ fGn RW1 RW1	1.44920	120.49734	377.00362	2.44167	698.28083
30	∅ fGn RW1 RW2	1.21710	97.66872	35.60251	1.61059	141.64119
31	∅ fGn RW2 RW2	0.13811	0.99573	0.08935	0.33026	0.70687
32	∅ RW1 RW1 RW1	1.12348	45.71516	132.64444	0.59712	60.69017
33	∅ RW1 RW1 RW2	0.67020	19.18436	39.54299	0.54059	15.96826
34	∅ RW1 RW2 RW2	14.16860	8821.25162	170560.29571	12.85950	100452.84085
35	∅ RW2 RW2 RW2	17.51650	7461.14435	72831.75736	12.47950	44566.17178
36	AR(1) AR(1) AR(1) AR(1)	0.02544	0.04314	0.63873	0.14618	0.09867
37	AR(1) AR(1) AR(1) fGn	0.03145	0.04049	0.04059	0.04170	0.03814
38	AR(1) AR(1) AR(1) RW1	0.01705	0.02889	0.07729	0.09577	0.05735
39	AR(1) AR(1) AR(1) RW2	0.01441	0.02387	0.01819	0.11273	0.03807
40	AR(1) AR(1) fGn fGn	0.03253	0.08202	0.56284	0.06370	0.14367
41	AR(1) AR(1) fGn RW1	0.03314	0.08926	0.64940	0.12355	0.25643
42	AR(1) AR(1) fGn RW2	0.03496	0.09883	0.48174	0.10397	0.13979
43	AR(1) AR(1) RW1 RW1	0.01525	0.01481	**0.01687**	0.05251	0.02348
44	AR(1) AR(1) RW1 RW2	0.01987	0.02683	0.12083	0.04197	0.03301
45	AR(1) AR(1) RW2 RW2	0.02569	0.03376	0.15744	0.12411	0.06571
46	AR(1) fGn fGn fGn	0.03572	0.10117	0.15990	0.05498	0.09996
47	AR(1) fGn fGn RW1	0.03413	0.07060	2.97383	0.05266	0.09897
48	AR(1) fGn fGn RW2	0.01928	0.03661	0.04589	0.04289	0.02211
49	AR(1) fGn RW1 RW1	0.01918	0.02352	0.01701	0.13995	0.05053
50	AR(1) fGn RW1 RW2	0.02206	0.05455	0.13965	0.13601	0.12660
51	AR(1) fGn RW2 RW2	0.02496	0.31923	0.09807	1.95341	1.05928
52	AR(1) RW1 RW1 RW1	0.01566	0.01641	0.13548	0.04746	0.02259
53	AR(1) RW1 RW1 RW2	0.01602	0.02684	0.05155	0.07635	0.04216
54	AR(1) RW1 RW2 RW2	0.01990	**0.01464**	0.03319	0.04819	**0.01189**
55	AR(1) RW2 RW2 RW2	0.02245	0.01709	0.02452	0.19415	0.04048
56	fGn fGn fGn fGn	0.03953	0.08946	0.22621	0.05853	0.07286
57	fGn fGn fGn RW1	0.03440	0.07176	0.92268	0.05716	0.05254
58	fGn fGn fGn RW2	0.01967	0.03866	0.06826	0.04884	0.03732
59	fGn fGn RW1 RW1	0.02046	0.02001	0.05828	0.04099	0.02081
60	fGn fGn RW1 RW2	0.01924	0.03988	0.05427	0.07883	0.02954
61	fGn fGn RW2 RW2	0.03169	1.61438	0.31585	128.11978	116.91836
62	fGn RW1 RW1 RW1	0.02034	0.01937	0.06995	0.08177	0.03282
63	fGn RW1 RW1 RW2	0.01947	0.02298	0.02594	0.05705	0.01845
64	fGn RW1 RW2 RW2	0.02639	0.01724	0.02205	0.04192	0.01489
65	fGn RW2 RW2 RW2	0.01446	0.02785	0.03574	48.60829	3.77382
66	RW1 RW1 RW1 RW1	1.37058	41.71948	442.91739	1.18783	5.10871
67	RW1 RW1 RW1 RW2	1.88309	22.74383	115.25862	1.38391	5.60507
68	RW1 RW1 RW2 RW2	0.77299	1576.89511	44678.18015	6.47930	2932.85075
69	RW1 RW2 RW2 RW2	1.96188	1.18509	1.77064	0.38131	0.73937
70	RW2 RW2 RW2 RW2	21.98333	1501.05794	57429.96521	12.62821	543.61378

Note: ∅ - Factor not included, AR(1) - First order autoregressive process, RW1 - First order random walk, RW2 - Second-order random walk, fGn - fractional Gaussian noise.

Table 9
Model Confidence Set - Bitcoin

Model	Rank_M	v_M	MCS_M	Rank_R	v_R	MCS_R	Loss
model_9	7	1.3766670	0.3374	8	1.6984847	0.3040	0.0004814428
model_18	8	1.4339879	0.3074	7	1.6205765	0.3498	0.0004702110
model_19	4	-1.6713485	1.0000	1	-0.4538497	1.0000	0.0004169703
model_38	9	1.7791717	0.1564	9	1.9494552	0.1882	0.0004756091
model_39	3	-1.7148126	1.0000	3	0.5686046	0.9422	0.0004196922
model_43	2	-1.8654228	1.0000	4	1.4349104	0.4622	0.0004330773
model_52	1	-2.7269143	1.0000	6	1.4922103	0.4268	0.0004416045
model_53	6	0.6125166	0.8380	5	1.4918914	0.4268	0.0004523332
model_65	5	-0.7358602	1.0000	2	0.4538497	0.9706	0.0004252128

Table 10
Model Confidence Set - ETH

Model	Rank_M	v_M	MCS_M	Rank_R	v_R	MCS_R	Loss
model_8	13	0.185606993	0.9966	16	5.3357107	0.0000	0.0008234438
model_9	1	-5.310248719	1.0000	7	2.2087581	0.1792	0.0006028546
model_18	14	0.688813624	0.8802	14	4.7323070	0.0000	0.0008731267
model_19	7	-2.352408624	1.0000	9	2.5999700	0.0618	0.0006591791
model_38	17	1.951391595	0.1874	17	5.3577610	0.0000	0.0010264780
model_39	10	-0.536828707	1.0000	15	4.7525109	0.0000	0.0007734321
model_43	4	-3.776364021	1.0000	1	-0.4937824	1.0000	0.0005110767
model_45	16	1.756303085	0.2780	5	2.0591009	0.2556	0.0021712232
model_49	11	-0.095054317	1.0000	11	3.4853356	0.0026	0.0008045881
model_52	2	-4.615663144	1.0000	2	0.4937824	0.9958	0.0005236851
model_54	8	-1.478440226	1.0000	4	1.7112573	0.4812	0.0006183204
model_55	6	-3.186752712	1.0000	3	1.2308460	0.8108	0.0006314626
model_59	5	-3.231446284	1.0000	8	2.2186601	0.1742	0.0006238311
model_62	3	-4.109271780	1.0000	6	2.0997222	0.2320	0.0006109515
model_63	9	-0.928695043	1.0000	13	4.1112156	0.0002	0.0007498049
model_64	12	0.002645169	1.0000	10	3.1366329	0.0112	0.0008101287
model_65	15	1.068479584	0.6836	12	3.9020456	0.0004	0.0009507113

Table 11
Model Confidence Set - XRP

Model	Rank_M	v_M	MCS_M	Rank_R	v_R	MCS_R	Loss
model_9	5	0.5488076	0.7770	4	2.2257112	0.0952	0.0007304257
model_19	6	0.8019862	0.5892	6	2.3180843	0.0710	0.0007569407
model_39	1	-6.6845351	1.0000	2	0.2232579	1.0000	0.0004779443
model_43	3	-2.6050644	1.0000	3	1.4821778	0.4752	0.0005084241
model_49	2	-4.6927726	1.0000	1	-0.2232579	1.0000	0.0004739967
model_55	4	0.4894977	0.8210	5	2.2383170	0.0912	0.0007281834
model_63	7	1.2653112	0.3198	7	2.4959426	0.0424	0.0008192075
model_64	8	1.3534522	0.2780	8	2.9950956	0.0104	0.0009775682

Table 12
Model Confidence Set - SOL

Model	Rank_M	v_M	MCS_M	Rank_R	v_R	MCS_R	Loss
model_1	7	-1.3430481	1.0000	9	1.6038853	0.8116	2.672726e-03
model_2	17	-1.3429951	1.0000	34	2.7136175	0.0586	3.328035e-03
model_3	10	-1.3430431	1.0000	15	2.1340078	0.4552	2.707899e-03
model_4	53	-1.3378636	1.0000	45	3.1339020	0.0098	1.199370e-01
model_5	51	-1.3382154	1.0000	16	2.1608512	0.2476	1.960128e-01
model_6	24	-1.3429397	1.0000	49	3.5195601	0.0012	4.108692e-03
model_7	33	-1.3427709	1.0000	51	3.5609599	0.0008	6.535468e-03
model_8	3	-1.3430777	1.0000	2	0.2309166	1.0000	2.371152e-03
model_9	1	-1.3430866	1.0000	1	-0.2309166	1.0000	2.331617e-03
model_10	15	-1.3430011	1.0000	37	2.8014776	0.0510	3.260394e-03
model_11	26	-1.3429331	1.0000	64	5.1509189	0.0000	4.285907e-03
model_12	13	-1.3430330	1.0000	42	3.0714500	0.0200	2.856684e-03
model_13	46	-1.3416828	1.0000	59	3.9753928	0.0000	3.267135e-02
model_14	48	-1.3412081	1.0000	41	3.0684065	0.0200	4.666727e-02
model_15	50	-1.3390038	1.0000	11	1.8334760	0.4552	2.344945e-01
model_16	18	-1.3429949	1.0000	35	2.7296640	0.0510	3.697796e-03
model_17	35	-1.3427284	1.0000	54	3.6953087	0.0002	7.712567e-03
model_18	14	-1.3430086	1.0000	30	2.5430188	0.0856	3.320340e-03
model_19	22	-1.3429574	1.0000	57	3.8495518	0.0002	4.124931e-03
model_20	31	-1.3427957	1.0000	48	3.3376266	0.0032	6.187107e-03
model_21	29	-1.3428814	1.0000	47	3.2298861	0.0066	5.371869e-03
model_22	39	-1.3425480	1.0000	40	2.9398341	0.0266	1.619662e-02
model_23	58	-1.3140092	1.0000	26	2.4376564	0.1158	8.043157e-01
model_24	63	-1.0761371	1.0000	22	2.4091818	0.1692	6.679574e+00
model_25	55	-1.3295936	1.0000	10	1.6222362	0.8116	1.166340e+00
model_26	21	-1.3429578	1.0000	25	2.4350138	0.1158	3.862806e-03
model_27	34	-1.3427316	1.0000	65	6.4295450	0.0000	7.195591e-03
model_28	6	-1.3430561	1.0000	3	0.9730128	1.0000	2.546653e-03
model_29	64	-0.8761844	1.0000	17	2.2100404	0.2476	1.117151e+01
model_30	61	-1.1696613	1.0000	32	2.5911439	0.0856	4.508765e+00
model_31	52	-1.3379038	1.0000	21	2.3491003	0.1692	1.832862e-01
model_32	57	-1.3214714	1.0000	23	2.4131351	0.1162	6.027672e-01
model_33	56	-1.3249691	1.0000	29	2.5280726	0.0944	4.740617e-01
model_34	66	1.3266086	0.1734	8	1.5629586	1.0000	7.754603e+02
model_36	47	-1.3415380	1.0000	56	3.7464574	0.0002	2.777015e-02
model_37	5	-1.3430591	1.0000	5	1.2580917	1.0000	2.555693e-03
model_38	41	-1.3424304	1.0000	62	4.1950337	0.0000	1.206802e-02
model_39	42	-1.3421821	1.0000	60	3.9959326	0.0000	1.695982e-02
model_40	30	-1.3428540	1.0000	36	2.7783733	0.0510	5.308734e-03
model_41	44	-1.3419099	1.0000	52	3.6075569	0.0006	1.985829e-02
model_42	38	-1.3425504	1.0000	38	2.8039986	0.0510	1.684580e-02
model_43	19	-1.3429751	1.0000	28	2.4636837	0.1158	3.763345e-03
model_44	4	-1.3430732	1.0000	7	1.4197300	1.0000	2.706110e-03
model_45	40	-1.3425138	1.0000	14	1.9785205	0.4552	2.966052e-02
model_46	23	-1.3429456	1.0000	43	3.1124987	0.0200	4.022990e-03
model_47	20	-1.3429659	1.0000	31	2.5805878	0.0856	3.744260e-03
model_48	9	-1.3430446	1.0000	12	1.8615138	0.4552	2.681227e-03
model_49	45	-1.3418658	1.0000	53	3.6772595	0.0002	2.682522e-02
model_50	43	-1.3419740	1.0000	44	3.1230819	0.0110	2.691695e-02
model_51	62	-1.1498827	1.0000	13	1.9475687	0.4552	7.567812e+00
model_52	12	-1.3430373	1.0000	24	2.4159583	0.1158	3.281959e-03
model_53	32	-1.3427800	1.0000	50	3.5334495	0.0010	8.277382e-03
model_54	8	-1.3430465	1.0000	20	2.2916893	0.2142	3.636811e-03
model_55	49	-1.3411402	1.0000	61	4.1483928	0.0000	4.884242e-02
model_56	28	-1.3429116	1.0000	46	3.2187668	0.0068	4.493713e-03
model_57	27	-1.3429254	1.0000	58	3.9426726	0.0000	4.305344e-03
model_58	16	-1.3429970	1.0000	27	2.4587401	0.1158	3.307855e-03
model_59	2	-1.3430790	1.0000	4	0.9783656	1.0000	2.514734e-03
model_60	37	-1.3426928	1.0000	66	6.4722289	0.0000	8.331428e-03
model_62	36	-1.3427071	1.0000	55	3.7087882	0.0002	9.275189e-03
model_63	25	-1.3429341	1.0000	63	5.1156060	0.0000	4.651388e-03
model_64	11	-1.3430392	1.0000	33	2.7129482	0.0856	3.462504e-03
model_66	59	-1.2542370	1.0000	19	2.2818592	0.2476	2.534057e+00
model_67	60	-1.2221051	1.0000	18	2.2760709	0.2476	3.515339e+00
model_69	54	-1.3345661	1.0000	39	2.8143315	0.0510	2.204406e-01
model_70	65	1.3213119	0.2002	6	1.3219883	1.0000	7.606004e+02

Table 13
Model Confidence Set - BNB

Model	Rank_M	v_M	MCS_M	Rank_R	v_R	MCS_R	Loss
model_1	17	-1.355337	1.0000	63	6.912292	0.0000	1.330234e-03
model_2	26	-1.355337	1.0000	66	7.774503	0.0000	2.626388e-03
model_3	19	-1.355337	1.0000	67	8.177092	0.0000	1.305383e-03
model_4	53	-1.355335	1.0000	24	2.668415	0.0878	2.039788e+00
model_5	55	-1.355331	1.0000	8	1.732315	0.5216	1.504726e+01
model_6	28	-1.355337	1.0000	65	7.603342	0.0000	2.906716e-03
model_7	29	-1.355337	1.0000	54	5.529041	0.0000	2.957364e-03
model_8	6	-1.355337	1.0000	46	4.952771	0.0000	5.961531e-04
model_9	2	-1.355337	1.0000	6	1.567928	1.0000	2.899257e-04
model_10	20	-1.355337	1.0000	61	6.096541	0.0000	1.446205e-03
model_11	18	-1.355337	1.0000	62	6.702830	0.0000	1.280079e-03
model_12	14	-1.355337	1.0000	58	5.904497	0.0000	1.108358e-03
model_13	51	-1.355336	1.0000	23	2.667111	0.3590	1.463236e+00
model_14	52	-1.355335	1.0000	22	2.522934	0.3590	1.808361e+00
model_15	59	-1.355248	1.0000	4	1.461052	1.0000	7.321673e+02
model_16	34	-1.355337	1.0000	45	4.911693	0.0000	4.846909e-03
model_17	33	-1.355337	1.0000	56	5.611240	0.0000	3.752396e-03
model_18	9	-1.355337	1.0000	47	5.015329	0.0000	6.140618e-04
model_19	4	-1.355337	1.0000	25	2.822938	0.0878	4.126275e-04
model_20	46	-1.355337	1.0000	40	4.328358	0.0002	4.230920e-02
model_21	41	-1.355337	1.0000	44	4.804334	0.0000	1.199151e-02
model_22	44	-1.355337	1.0000	37	3.793942	0.0010	2.865767e-02
model_23	62	-1.344557	1.0000	16	2.037332	0.3590	1.312828e+04
model_24	65	-1.294353	1.0000	13	2.019136	0.3590	7.184999e+04
model_25	54	-1.355332	1.0000	5	1.531779	1.0000	2.473968e+01
model_26	37	-1.355337	1.0000	51	5.173814	0.0000	9.057800e-03
model_27	35	-1.355337	1.0000	57	5.620866	0.0000	5.378980e-03
model_28	7	-1.355337	1.0000	27	3.233904	0.0140	5.754397e-04
model_29	66	1.003176	0.7430	9	1.900714	0.5216	1.334398e+06
model_30	64	-1.314234	1.0000	12	2.011280	0.3590	4.934253e+04
model_31	48	-1.355337	1.0000	14	2.024406	0.3590	1.075924e+00
model_32	61	-1.348118	1.0000	15	2.036994	0.3590	8.911604e+03
model_33	60	-1.354817	1.0000	19	2.164322	0.3590	5.589657e+02
model_36	38	-1.355337	1.0000	43	4.540663	0.0000	1.158839e-02
model_37	24	-1.355337	1.0000	60	6.092628	0.0000	1.674476e-03
model_38	32	-1.355337	1.0000	53	5.493326	0.0000	3.750334e-03
model_39	22	-1.355337	1.0000	55	5.577414	0.0000	1.710776e-03
model_40	45	-1.355337	1.0000	42	4.528339	0.0000	2.356340e-02
model_41	47	-1.355337	1.0000	38	3.966923	0.0002	7.894017e-02
model_42	43	-1.355337	1.0000	33	3.578170	0.0014	2.537978e-02
model_43	12	-1.355337	1.0000	34	3.592593	0.0012	7.449666e-04
model_44	15	-1.355337	1.0000	29	3.382989	0.0032	1.491588e-03
model_45	31	-1.355337	1.0000	10	1.922399	0.5216	1.010973e-02
model_46	40	-1.355337	1.0000	49	5.090055	0.0000	1.113855e-02
model_47	39	-1.355337	1.0000	48	5.055904	0.0000	1.101094e-02
model_48	10	-1.355337	1.0000	41	4.341914	0.0002	6.078916e-04
model_49	27	-1.355337	1.0000	28	3.365976	0.0042	3.454116e-03
model_50	42	-1.355337	1.0000	26	3.120530	0.0140	2.283506e-02
model_51	50	-1.355336	1.0000	11	1.964790	0.3590	2.488936e+00
model_52	11	-1.355337	1.0000	35	3.616730	0.0010	7.261974e-04
model_53	25	-1.355337	1.0000	39	4.311022	0.0002	2.221039e-03
model_54	1	-1.355337	1.0000	1	-1.288985	1.0000	2.229073e-04
model_55	21	-1.355337	1.0000	30	3.413971	0.0028	2.159030e-03
model_56	36	-1.355337	1.0000	52	5.340904	0.0000	5.952179e-03
model_57	30	-1.355337	1.0000	50	5.093001	0.0000	3.158903e-03
model_58	23	-1.355337	1.0000	59	6.087298	0.0000	1.603294e-03
model_59	8	-1.355337	1.0000	31	3.420599	0.0028	6.317763e-04
model_60	13	-1.355337	1.0000	64	7.580321	0.0000	1.053541e-03
model_61	63	-1.341040	1.0000	7	1.607075	1.0000	4.745167e+04
model_62	16	-1.355337	1.0000	36	3.739144	0.0010	1.407994e-03
model_63	5	-1.355337	1.0000	32	3.529675	0.0028	4.903075e-04
model_64	3	-1.355337	1.0000	20	2.248234	0.3590	4.276350e-04
model_65	56	-1.355315	1.0000	68	19.854833	0.0000	1.432483e+01
model_66	57	-1.355286	1.0000	18	2.140132	0.3590	5.860597e+01
model_67	58	-1.355277	1.0000	17	2.120961	0.3590	7.181775e+01
model_68	68	1.341346	0.3088	3	1.343737	1.0000	5.575299e+07
model_69	49	-1.355336	1.0000	21	2.416521	0.3590	9.983960e-01
model_70	67	1.247098	0.5354	2	1.288985	1.0000	2.273045e+06

6. Conclusion

In this work, we introduce a new class of multivariate models of multi-factor stochastic volatility, allowing a latent factor structure based on distinct memory processes, enabling the presence of first and second order Random-walk processes and long memory processes in the factor dynamics latent processes, in addition to autoregressive processes that are usually used in stochastic volatility models. This structure allows capturing some stylized facts relevant in modeling conditional volatility processes. RW1 processes are used to capture the effects of shocks with permanent effects on the level of conditional volatility, and the second-order version of this process (RW2) is a way of approximating smooth changes in the level of volatility, being analogous to a spline representation for smooth and permanent changes in the mean latent conditional variance.

The proposed generalization also allows latent factors to have long-memory dynamics, represented by fractional Gaussian noise processes. This dynamic is observed in conditional volatility series, and has recently been reinterpreted as trending fractional volatility processes (Comte and Renault, 1998; Comte et al., 2012; Alòs and Yang, 2017), through fractional Brownian motion with Hurst parameter H>.5. Our model allows for multivariate volatility processes with a possible mix of latent factors with distinct H parameters. These classes of processes have been demonstrated to be important for capturing patterns of dependence on realized volatility and implied volatility with relevant impacts on asset pricing and risk management.

The results of the empirical analyzes for the cryptocurrency market indicate the relevance of including alternative processes to autoregressive processes in the dynamics of latent factors. The model selection procedures and in-sample and out-of-sample fit measures indicate the relevance of the processes RW1, RW2 and the long memory process fGn for modeling the joint dynamics of conditional variance in financial assets, providing empirical support the application of the new methodology of multivariate stochastic volatility models proposed in this work.

Author Contributions: These authors contributed equally to this work.

Funding: The authors acknowledge funding from Capes, CNPq (310646/2021-9) and FAPESP (2023/02538-0).

Data Availability Statement: All data taken from coinmarketcap.com, accessed on 31 November 2023.

Conflicts of Interest: The authors declare no conflicts of interest.

References

Aharon, D. Y., Butt, H. A., Jaffri, A. and Nichols, B. (2023). Asymmetric volatility in the cryptocurrency market: New evidence from models with structural breaks, *International Review of Financial Analysis* **87**: 102651. **URL:** https://www.sciencedirect.com/science/article/pii/S1057521923001679

Alòs, E. and Yang, Y. (2017). A fractional heston model with H>1/2, *Stochastics* **89**(1): 384–399.

Andersen, T. and Sorensen, B. (1996). GMM estimation of a stochastic volatility model: a Monte Carlo study, *Journal of Business & Economic Statistics* **14**(3): 328–352.

Ardia, D., Bluteau, K. and Rüede, M. (2019). Regime changes in bitcoin garch volatility dynamics, *Finance Research Letters* **29**: 266–271. **URL:** https://www.sciencedirect.com/science/article/pii/S1544612318303970

Asai, M., McAleer, M. and Yu, J. (2006). Multivariate stochastic volatility: A review, *Econometric Reviews* **25**(2-3): 145–175.

Audrino, F. and Bühlmann, P. (2009). Splines for financial volatility, *Journal of the Royal Statistical Society. Series B (Statistical Methodology)* **71**(3): 655–670.

Bayer, C., Friz, P. K., Gassiat, P., Martin, J. and Stemper, B. (2020). A regularity structure for rough volatility, *Mathematical Finance* **30**(3): 782–832. **URL:** https://onlinelibrary.wiley.com/doi/abs/10.1111/mafi.12233

Beran, J. (2017). *Statistics for long-memory processes*, Routledge.

Beran, J., Schützner, M. and Ghosh, S. (2010). From short to long memory: Aggregation and estimation, *Computational Statistics & Data Analysis* **54**(11): 2432–2442.

Breidt, F. J., Crato, N. and De Lima, P. (1998). The detection and estimation of long memory in stochastic volatility, *Journal of Econometrics* **83**(1-2): 325–348.

Chaim, P. and Laurini, M. P. (2018). Volatility and return jumps in bitcoin, *Economics Letters* **173**: 158–163.
URL: https://www.sciencedirect.com/science/article/pii/S0165176518304245

Chaim, P. and Laurini, M. P. (2019a). *Essays in Financial Econometrics*, Phd dissertation in applied economics, Faculdade de Economia, Administração e Contabilidade de Ribeirão Preto, Ribeirão Preto.

Chaim, P. and Laurini, M. P. (2019b). Nonlinear dependence in cryptocurrency markets, *The North American Journal of Economics and Finance* **48**: 32–47.
URL: https://www.sciencedirect.com/science/article/pii/S1062940818303553

Chevallier, J. and Sanhaji, B. (2023). Jump-robust realized-garch-midas-x estimators for bitcoin and ethereum volatility indices, *Stats* **6**(4): 1339–1370.
URL: https://www.mdpi.com/2571-905X/6/4/82

Comte, F., Coutin, L. and Renault, É. (2012). Affine fractional stochastic volatility models, *Annals of Finance* **8**(2–3): 337–378.

Comte, F. and Renault, É. (1998). Long memory in continuous-time stochastic volatility models, *Mathematical Finance* **8**(4): 291–323.

Engle, R. (1982). Autoregressive Conditional Heteroskedasticity with estimates of the variance of United Kingdom inflation, *Econometrica* **50**(4): 987–1007.

Engle, R. F. and Rangel, J. G. (2008). The spline-garch model for low-frequency volatility and its global macroeconomic causes, *The Review of Financial Studies* **21**(3): 1187–1222.

Fengler, M. R. (2009). Arbitrage-free smoothing of the implied volatility surface, *Quantitative Finance* **9**(4): 417–428.
URL: https://doi.org/10.1080/14697680802595585

Gatheral, J., Jaisson, T. and Rosenbaum, M. (2018). Volatility is rough, *Quantitative Finance* **18**(6): 933–949.

Granger, C. W. (1980). Long memory relationships and the aggregation of dynamic models, *Journal of econometrics* **14**(2): 227–238.

Haldrup, N. and Valdés, J. E. V. (2017). Long memory, fractional integration, and cross-sectional aggregation, *Journal of econometrics* **199**(1): 1–11.

Hansen, P. R., Lunde, A. and Nason, J. M. (2011). The model confidence set, *Econometrica* **79**(2): 453–497.

Harvey, A. C. (1998). Stochastic volatility models with long memory, *in* J. Knight and E. Satchell (eds), *Forecasting Volatility in Financial Markets*, Butterworth-Haineman, London, pp. 307–320.

Harvey, A. C. and Jaeger, A. (1993). Detrending, stylized facts and the business cycle, *Journal of Applied Econometrics* **8**(3): 231–247.

Harvey, A. and Trimbur, T. (2008). Trend estimation and the Hodrick-Prescott filter, *Journal of the Japan Statistical Society* **38**(1): 41–49.

Harvey, A., Ruiz, E. and Shephard, N. (1994). Multivariate stochastic variance models, *The Review of Economic Studies* **61**(2): 247–264.

Hosking, J. R. M. (1981). Fractional differencing, *Biometrika* **68**(1): 165–176.

Jacquier, E., Polson, N. and Rossi, P. (1995). Models and priors for multivariate stochastic volatility, *Technical report*, Centre Interuniversitaire de Recherche en Analyse des Organisations (CIRANO).

Kastner, G. and Frühwirth-Schnatter, S. (2014). Ancillarity-sufficiency interweaving strategy (ASIS) for boosting MCMC estimation of stochastic volatility models, *Computational Statistics & Data Analysis* **76**(1): 408–423.

Kim, S. and Shephard, N. (1998). Stochastic volatility: likelihood inference and comparison with ARCH models, *The Review of Economic Studies* **65**(3): 361–393.

Laurini, M. P. (2011). Imposing no-arbitrage conditions in implied volatilities using constrained smoothing splines, *Applied Stochastic Models in Business and Industry* **27**(6): 649–659.
URL: https://onlinelibrary.wiley.com/doi/abs/10.1002/asmb.877

Laurini, M. P. and Hotta, L. K. (2017). Gmc/gel estimation of stochastic volatility models, *Communications in Statistics - Simulation and Computation* **46**(9): 6828–6844.
URL: https://doi.org/10.1080/03610918.2016.1213282

Lindgren, F. and Rue, H. (2008). On the second-order random walk model for irregular locations, *Scandinavian Journal of Statistics* **35**(4): 691–700.

Mandelbrot, B. B. and Van Ness, J. W. (1968). Fractional brownian motions, fractional noises and applications, *SIAM Review* **10**(4): 422–437.

Martino, S. (2007). Approximate Bayesian inference for multivariate stochastic volatility models, *Technical report*, Department of Mathematical Sciences, Norwegian University of Science and Technology, Trondheim, Norway.

Martino, S., Aas, K., Lindqvist, O., Neef, L. and Rue, H. (2011). Estimating stochastic volatility models using integrated nested Laplace approximations, *European Journal of Finance* **17**(7): 487–503.

Nacinben, J. P. C. d. S. M. and Laurini, M. (2024). Multivariate stochastic volatility modeling via integrated nested laplace approximations: A multifactor extension, *Econometrics* **12**(1).
URL: https://www.mdpi.com/2225-1146/12/1/5

Nelson, D. (1988). *The time series behavior of stock market volatility and returns*, Doutorado em economia, Massachusetts Institute of Technology, Cambridge.

Paige, R. L. and Trindade, A. A. (2010). The Hodrick-Prescott Filter: A special case of penalized spline smoothing, *Electronic Journal of Statistics* **4**: 856–874.

Quintana, J. and West, M. (1987). An analysis of international exchange rates using multivariate DLM's, *Journal of the Royal Statistical Society: Series D (The Statistician)* **36**(2-3): 275–281.

Robert, C. (2001). *The Bayesian Choice: From Decision-Theoretic Foundations to Computational Implementation*, Springer.

Rue, H. and Held, L. (2005). *Gaussian Markov random fields: Theory and applications*, CRC Press.

Rue, H. and Martino, S. (2007). Approximate Bayesian inference for hierarchical Gaussian Markov random field models, *Journal of Statistical Planning and Inference* **137**(10): 3177–3192.

Rue, H., Martino, S. and Chopin, N. (2009). Approximate Bayesian inference for latent gaussian models by using integrated nested Laplace approximations, *Journal of the Royal Statistical Society* **71**(2): 319–392.

Shi, S., Yu, J. and Zhang, C. (2022). Fractional gaussian noise: Spectral density and estimation methods. Working Paper.

Simpson, D., Rue, H., Riebler, A., Martins, T. G. and Sørbye, S. H. (2017). Penalising Model Component Complexity: A Principled, Practical Approach to Constructing Priors, *Statistical Science* **32**(1): 1 – 28.
URL: https://doi.org/10.1214/16-STS576

Sørbye, S. H., Myrvoll-Nilsen, E. and Rue, H. (2017). An approximate fractional Gaussian noise model with $\mathcal{O}(n)$ computational cost, *Statistics and Computing* pp. 1–13.

Taylor, S. (1986). *Modelling Financial Time Series*, John Wiley & Sons, Hoboken.

Valente, F. and Laurini, M. (2024). Bayesian inference for long memory term structure models, *Journal of Statistical Computation and Simulation* **0**(0): 1–25.
URL: https://doi.org/10.1080/00949655.2023.2299938

Vasicek, O. A. and Fong, H. G. (1982). Term structure modeling using exponential splines, *The Journal of Finance* **37**(2): 339–348.

Vieira, L. I. and Laurini, M. P. (2023). Time-varying higher moments in bitcoin, *Digital Finance* **5**: 231–260.
URL: https://doi.org/10.1007/s42521-022-00072-8

Watanabe, S. (2010). Asymptotic equivalence of bayes cross validation and widely applicable information criterion in singular learning theory, *Journal of Machine Learning Research* **11**: 3571–3594.
verland Bergsli et al.

Øverland Bergsli, L., Lind, A. F., Molnár, P. and Polasik, M. (2022). Forecasting volatility of bitcoin, *Research in International Business and Finance* **59**: 101540.
URL: https://www.sciencedirect.com/science/article/pii/S0275531921001616